

---

# Structured Graph Variational Autoencoders for Indoor Furniture layout Generation

---

**Aditya Chattopadhyay \***  
Department of Computer Science  
Johns Hopkins University  
achatto1@jhu.edu

**Xi Zhang**  
Amazon.com, Inc.  
xizhn@amazon.com

**David Paul Wipf**  
Amazon.com, Inc.  
daviwipf@amazon.com

**Rene Vidal**  
Amazon.com, Inc.  
rvidal@amazon.com

**Himanshu Arora**  
Amazon.com, Inc.  
arorah@amazon.com

## Abstract

We present a structured graph variational autoencoder for generating the layout of indoor 3D scenes. Given the room type (e.g., living room or library) and the room layout (e.g., room elements such as floor and walls), our architecture generates a collection of objects (e.g., furniture items such as sofa, table and chairs) that is consistent with the room type and layout. This is a challenging problem because the generated scene should satisfy multiple constraints, e.g., each object must lie inside the room and two objects cannot occupy the same volume. To address these challenges, we propose a deep generative model that encodes these relationships as soft constraints on an attributed graph (e.g., the nodes capture attributes of room and furniture elements, such as class, pose and size, and the edges capture geometric relationships such as relative orientation). The architecture consists of a graph encoder that maps the input graph to a structured latent space, and a graph decoder that generates a furniture graph, given a latent code and the room graph. The latent space is modeled with auto-regressive priors, which facilitates the generation of highly structured scenes. We also propose an efficient training procedure that combines matching and constrained learning. Experiments on the 3D-FRONT dataset show that our method produces scenes that are diverse and are adapted to the room layout.

## 1 Introduction

The last few years have seen significant advances in image generation powered by the emergence of deep generative models such as GANs Goodfellow et al. (2014) and VAEs Kingma and Welling (2014). State-of-the-art methods are able to generate images of a single object category (e.g., faces) with amazingly realistic quality (e.g., Karras et al. (2020)). However, the problem of generating images of complex scenes composed of multiple objects in diverse arrangements remains a challenge. As an example, images of indoor scenes consist of room elements (floor, walls, etc.) and furniture items (table, chairs, beds, night stands) arranged in different ways depending on the room type (living room, bedroom, etc.) and style (elegant, contemporary, etc.). Moreover, room elements and furniture items should satisfy geometric and stylistic constraints, e.g., each object must lie inside the room and on the floor, two objects cannot occupy the same volume, some objects tend to co-occur in particular orientations relative to the room layout.

---

\*This work was done during Aditya's internship with Amazon

Recent work on indoor scene image generation Gadde u. a. (2021) aims to address the challenge of generating complex indoor scenes by using GANs with multiple discriminators that specialize in localizing different objects within an image. By adding a “broker” to mediate among such discriminators, Gadde u. a. (2021) achieves state-of-the-art results on synthesizing images of living rooms. However, such state-of-the-art image generation models are far from capturing rich structure in their latent spaces to allow for image generation that is conditioned on rich structures. For example, given an image of a scene with a few objects, how can we generate other images of the same scene, but with additional objects that are consistent with previous objects? We contend that addressing such complex image generation problems requires reasoning about the content of the scene in 3D space.

As a stepping stone, this paper focuses on the problem of conditional generation of the scene’s 3D layout, rather than a 2D image, though we can synthesize images using a renderer given the layout. Specifically, we assume we are given the room type (e.g., living room or library room) and the room layout (e.g., room elements such as floor and walls), and our goal is to generate a collection of objects (e.g., furniture items such as sofa, coffee table and chairs) that is consistent with the room type and layout. For example, if the input room is larger, we expect the objects to be larger or more spread out. Moreover, we expect the generator to synthesize diverse object arrangements for the same room, and we expect such arrangements to satisfy the aforementioned geometric and stylistic constraints.

Recent work on scene graph generation Armeni u. a. (2019); Wang u. a. (2018); Keshavarzi u. a. (2020) aims to address these challenges using supervision in the form of scene hierarchies or relational graphs. However, the contextual space of possible arrangements objects in a room is simply too large to be modeled using hand-crafted heuristics or hierarchies. This has led to recent efforts on training networks directly from data, e.g., autoregressive models based on CNNs Ritchie u. a. (2019) or Transformers Wang u. a. (2020); Paschalidou u. a. (2021). However, we argue that latent variable models offer several advantages relative to autoregressive models. Firstly, they often lead to a more interpretable latent structure and allow the user to manipulate the generated samples by intervening in the latent space Higgins u. a. (2016); Kumar u. a. (2017). For example, given a room, one could manipulate the latent space to recommend furniture in a “similar” looking room. Such manipulations are not easy to implement in autoregressive models, which directly learn the conditional distribution of furniture items conditioned on other items. Secondly, the latent space learnt by VAEs is often useful in downstream semi-supervised or supervised classification Kingma u. a. (2014). For instance one might be interested in classifying interior rooms based on style (modern, contemporary, minimalist, traditional) without access to fine-grained level annotations at scale.

In this work, we propose a latent-variable model called Structured Graph Variational Autoencoders for the purpose of generating indoor 3D scenes. In our model, we represent both the room and furniture layouts with an attributed graph whose nodes correspond to room elements or furniture items, node attributes encode object class, position, orientation, etc., and, edges correspond to relationships among nodes captured by edge attributes such as relative orientation. We then propose a scene generative model consisting of a graph encoder that maps the input graph to a latent space, and a graph decoder that generates a furniture graph, given a latent code and the room graph. Specifically, we make the following contributions:

1. *A structured auto-regressive prior for graphs:* This is our main contribution. Contemporary graph-VAE architectures typically encode the graph into a single latent vector and then use a multi-layered perceptron (MLP) to decode it back to a graph Simonovsky und Komodakis (2018); Kipf und Welling (2016a). These architectures are known to be insufficient for learning indoor 3D scenes Para u. a. (2021). In contrast, we propose to have a separate latent code for each furniture item. This has been previously explored in Luo u. a. (2020). However, in that work the authors assume that each furniture is associated with a latent which is sampled i.i.d from a standard Gaussian distribution. We argue that this assumption is limiting for the purpose of indoor scene synthesis especially when the underlying graph is complete and the decoder is a message passing GNN. To remedy this, we propose a novel autoregressive prior based on linear Gaussian models and propose an efficient way to compute the KL divergence term in the VAE objective. This requires a matching procedure since there is no canonical ordering of graph nodes.
2. *Learning graph-VAEs under constraints:* To facilitate learning, we use simple intuitive constraints like limiting the relative distances between furniture items, such as a chair and a table. These can be easily computed from training data. We then train our VAE model

end-to-end under these constraints utilizing the recently introduced constrained learning framework by Chamon und Ribeiro (2020). We not in passing that Para *et al.* Para u. a. (2021) also employ constraints for synthesizing plausible indoor scenes. Their approach however is only limited to linear constraints and training is not end-to-end.

3. *Experimental evaluation:* Through extensive experiments we show that our proposed model is competitive with the state of the art at indoor scene synthesis. Moreover, we leverage the information captured by our latent code to propose furniture layouts to “similar” looking rooms or interpolate gracefully between two given furnished rooms. We also show, via ablation studies, that our proposed model is better at capturing co-occurrence distributions between object categories than baseline graph VAE architectures.

## 2 Related Work

**Graph-based inference:** Graphical representation of scenes and graph-based inference has been extensively studied in the past. Early works Fisher u. a. (2012, 2011); Yeh u. a. (2012); Jiang u. a. (2018); Qi u. a. (2018) employed “shallow” methods like hand-crafted graph kernels or probabilistic graphical models to learn the furniture arrangements. Recent works leverage deep generative models to learn good scene representations directly from spatial data. The community has explored avenues for combining graphs with VAEs to synthesize 3D scenes Li u. a. (2019); Zhang u. a. (2020); Luo u. a. (2020). However, all these methods rely on external annotations besides just the object labels and their spatial bounding boxes. For instance, Luo u. a. (2020) relies on user-defined scene-graphs as input, Li u. a. (2019) requires hand-crafted hierarchies, and Purkait u. a. (2020) uses heuristics to extract context-free grammars from data which are then used to train a grammar-VAE Kusner u. a. (2017). Our proposed VAE is different from all these methods in that we would like to learn these rules directly from data which requires modelling of a structured prior distribution. On the other hand, Wang *et al.* Wang u. a. (2019) uses graphs for high-level planning of the furniture layout of the room in a 2-stage approach where they train a generator to synthesize scene graphs followed by a CNN to propose consistent furniture poses. Their model has no latent variables and is slower due to the 2-stage process.

**Autoregressive Scene Generation.** Recent successful models for indoor scene synthesis are all autoregressive in nature Wang u. a. (2018); Ritchie u. a. (2019); Wang u. a. (2020); Paschalidou u. a. (2021). Wang *et al.* Wang u. a. (2020) introduced an autoregressive scene generation pipeline, Sceneformer, using multiple transformers Vaswani u. a. (2017) which predict objects’ category, location and size separately. Concurrently, FastSynth Ritchie u. a. (2019) introduced a similar pipeline, where the authors train separate CNNs based on a top-down representation of the scene to sequentially insert objects into the scene. Their method however requires auxiliary supervision in the form of depth and semantic segmentation maps. Another recent transformer-based autoregressive approach was proposed in Paschalidou u. a. (2021), which replaces the multiple trained models of past works with a single unified model. Unlike these models, we learn an end-to-end latent variable model to generate 3D indoor scenes trained from spatial data.

**Expressive latent distributions for VAEs.** There has been extensive work into designing expressive distributions for VAEs. For example, Klushyn u. a. (2019) proposes a hierarchical prior, Rezende und Mohamed (2015) uses normalizing flows to model a more expressive posterior distribution over latents, Chen u. a. (2016) uses an autoregressive prior, and Tomczak und Welling (2018) advocates the use of a mixture distribution for the prior based on the posterior distribution of the encoder. However, learning expressive distributions for latent spaces which are expressed as graphs is challenging due to the absence of any canonical ordering between the different nodes of a graph. This makes computing the required KL divergence term in the ELBO notoriously difficult. In this work we propose to model the latent space as an autoregressive linear Gaussian model which allows us to formulate the ordering as a Quadratic Assignment problem for which we also propose an efficient approximation.

## 3 Our Approach

This section describes the proposed Structure Graph Variational Autoencoder model. First, we describe how we represent the 3D scene layout with an attributed graph. Next, we describe the SG-VAE architecture. The VAE encoder is a GNN that processes the graph and produces latent variables which are then passed to another GNN which serves as the VAE decoder. Then, we describe how we

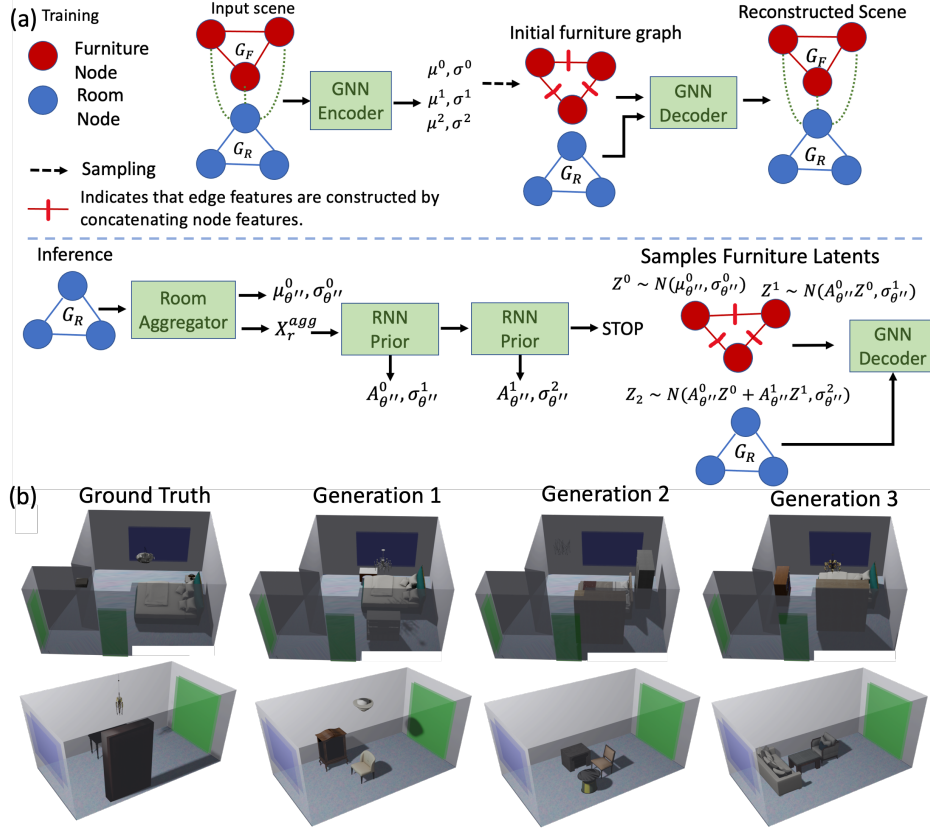


Figure 1: (a) **Overview of the proposed model.** The input scene graph includes the furniture and room sub-graphs and is complete (we omit depicting certain edges to prevent clutter). The Encoder predicts a mean and variance per furniture node, which are then used to sample latents for proposing furniture nodes by the decoder. During inference we use the proposed autoregressive prior to generate the latents, which are then subsequently processed by the decoder for scene synthesis; (b) **Generated scenes.** Sample generations for our model for a bedroom (row 1) and a library (row 2). Green rectangles indicate doors while blue rectangles indicate windows

parameterize the prior on the latent space using an autoregressive model which is learnt. Finally, we describe the proposed training methodology, which includes some constraints for faster convergence. A schematic depiction of our approach is given in Figure 1a. We share more architectural and feature engineering details in the Appendix.

### 3.1 Indoor scene representation as a graph

We represent an indoor scene as an attributed graph  $G = (V, E, X)$ . Here the nodes  $V$  denote room layout components (floor, wall, windows) and furniture items (sofa, chair, bed), the edges  $E \subseteq V \times V$  denote relationships between the nodes (e.g., sofa parallel to wall), and the attributes  $X$  denote features associated with the nodes and edges (e.g., location of furniture items or relative orientation between bed and wall). The graph has two node types (room nodes  $V_R$ , furniture nodes  $V_F$ ), three edge types (room-room edges  $E_{RR}$ , room-furniture edges  $E_{RF}$  and furniture-furniture edges  $E_{FF}$ ), and five attribute types corresponding to these node and edge types ( $X_R, X_F, X_{RR}, X_{RF}$  and  $X_{FF}$ ). In this work, we consider the graph as complete, that is,  $E_{RF} = V_R \times V_F$ ,  $E_{FF} = V_F \times V_F$  and  $E_{RR} = V_R \times V_R$ .

We will identify two main subgraphs of  $G$ . The room layout graph  $G_R = (V_R, E_R, X_R, X_{RR})$  consists of  $n_R := |V_R|$  nodes (or room elements) and  $e_R := |E_R|$  edges, where the node attributes  $X_R \in \mathbb{R}^{n_R \times d_R}$  denote the class, location, orientation and size of the room element, and the edge attributes  $X_{RR} \in \mathbb{R}^{e_R \times d_{RR}}$  encode geometric or functional relationships between two room elements (relative location, relative orientation etc.). The room type  $T$  is also encoded as a categorical feature



into  $X_R$ . Similarly, the furniture layout graph  $G_F = (V_F, E_F, X_F, X_{FF})$  consists of  $n_F := |V_F|$  nodes (or furniture items) and  $e_F = |E_F|$  edges, where the node attributes  $X_F \in \mathbb{R}^{n_F \times d_F}$  denote the class of the furniture item, its location, orientation, size, color, and its 3D shape descriptor, and its edge attributes  $X_{FF} \in \mathbb{R}^{e_F \times d_{FF}}$  encode geometric or functional relationships between two furniture items. We obtain the shape descriptors of each furniture item by processing a 3D point cloud of the item through PointNet Qi u. a. (2017) pretrained on the Stanford ShapeNet dataset Chang u. a. (2015).

### 3.2 Proposed Generative Model

We would like to design and learn a probabilistic model  $p(G_F | G_R, T, n_F)$  that generates a furniture layout  $G_F$  given the room layout  $G_R$ , type  $T$  (say, bedroom or library room) and number of furniture items  $n_F$  to place in the room. We assume there exists latent  $Z$  such that

$$p(G_F | G_R, T, n_F) = \int p(G_F | Z, n_F, G_R, T) p(Z | n_F, G_R, T) dZ. \quad (1)$$

Our proposed model consists of three main ingredients:

1. An encoder,  $q_\phi(Z | G, T, n_F)$ , which maps both room and furniture layouts ( $G_R$  and  $G_F$  resp.) as well as room type and number of furniture items to a latent variable  $Z$ , which captures the diversity of room-aware furniture layouts. The parameters of the encoder are denoted as  $\phi$ .
2. A decoder,  $p_{\theta'}(G_F | Z, n_F, G_R, T)$ , which maps the number of furniture items, the latent variable as well as the room layout and type to a furniture layout. The parameters of the encoder are denoted as  $\theta'$ .
3. A prior model  $p_{\theta''}(Z | n_F, G_R, T)$ . The difference between the prior model and the encoder is that the prior model only considers the room layout  $G_R$  and not  $G$ . The parameters of the prior model are denoted as  $\theta''$ .

The encoder, decoder and prior model are parameterized with GNNs which we will describe in the next subsection.

Given a training set, consisting of indoor scenes in the form of attributed graphs  $\mathcal{G} = \{G_1, G_2, \dots, G_n\}$ , we learn the parameters  $\{\theta', \theta'', \phi\}$  by optimizing the following empirical average over the training set:

$$\mathcal{L}(\theta', \theta'', \phi) = \frac{1}{n} \sum_{i=1}^n \mathcal{L}(G_i, \theta', \theta'', \phi), \quad (2)$$

where, for any  $G \in \mathcal{G}$ ,  $L(G, \theta', \theta'', \phi)$  denotes the Evidence Lower Bound (ELBO) defined as:

$$\begin{aligned} \mathcal{L}(G, \theta', \theta'', \phi) = & \mathbb{E}_{Z \sim q_\phi(Z | G, T, n_F)} [\log p_{\theta'}(G_F | Z, n_F, G_R, T)] \\ & - KL(q_\phi(Z | G, T, n_F) || p_{\theta''}(Z | n_F, G_R, T)). \end{aligned} \quad (3)$$

As mentioned in section 1, we optimize (2) under constraints to speed up convergence, as we will describe in subsection 3.3.

**Graph Encoder.** The encoder models the approximate posterior of a latent variable  $Z$  given  $(G, T, n_F)$ . We assume that the distribution of  $Z$ ,  $q_\phi(Z | G, T, n_F)$ , is Gaussian with mean  $\mu_\phi(G, T, n_F)$  and a diagonal covariance matrix with diagonal entries  $\sigma_\phi(G, T, n_F)$ . The distribution parameters  $(\mu_\phi, \sigma_\phi)$  are modeled as the output of an attention-based message passing graph neural network (MP-GNN) with weights  $\phi$ . The design of the MP-GNN is inspired by Mavroudi u. a. (2020), where each layer  $l = 1, \dots, L$  of the MP-GNN maps a graph  $G^{l-1}$  to another graph  $G^l$  by updating the graph's node and edge features. Specifically, let  $h_i^l$  and  $h_{ij}^l$  denote the features of node  $i$  and edge  $(i, j)$  of graph  $G^l$ , respectively. Let the input to the network be the graph  $G^0 = G$ , so that  $h_i^0$  and  $h_{ij}^0$  denote the node features (rows of  $X_R$  and  $X_F$ ) and edge features (rows of  $X_{RR}$ ,  $X_{FF}$  and  $X_{RF}$ ), respectively. At each iteration of node and edge refinement, the MP-GNN: (1) adapts the scalar edge weights by using an attention mechanism; (2) updates the edge attributes depending on the edge type, the attention-based edge weights, the attributes of the connected nodes and the previous edge attribute; and (3) updates the node attribute by aggregating attributes from incoming edges.

After  $L$  layers of refinement, we obtain a graph  $G^L$ , whose node features are mapped via a linear layer with weights  $W_\mu, W_\sigma$  to obtain the parameters of the Gaussian model as  $\mu_\phi^i(G, T) =$

$W_\mu h_i^L$ ,  $\sigma_\phi^i(G, T) = \exp(W_\sigma h_i^L)$  where  $i = 1, \dots, n_F$ . Note that there is a different Gaussian for each node of the graph. Therefore, the output of the encoder will be two matrices  $\mu_\phi(G, T, S) \in \mathbb{R}^{n_F \times d_F}$  and  $\sigma_\phi(G, T, S) \in \mathbb{R}^{n_F \times d_F}$  corresponding to the mean and standard deviation vectors of the latent variable matrix  $Z \in \mathbb{R}^{n_F \times d_F}$ .

**Graph Decoder.** The decoder maps  $(n_F, Z)$  and the room layout, type  $(G_R, T)$  to a desired furniture layout via the distribution  $p_{\theta'}(G_F | Z, n_F, G_R, T)$ . The generative process proceeds as follows,

An initial fully connected furniture graph  $G_F^0$  instantiated. Each node of  $G_F^0$  is associated with a feature of dimension  $d_F$  corresponding to one of the rows of  $Z$ . Each edge  $(i, j)$  of  $G_F^0$  of type  $\epsilon \in \{RF, FF\}$  is associated with a feature  $Z_{ij} = (Z_i, Z_j)$  as the concatenation of the node features. As a result, we obtain an initial graph  $G_0$  that includes both the initial furniture graph  $G_F^0$  as well as the given room graph  $G_R$  as subgraphs. The initial graph  $G_0$  is passed to a MP-GNN, which follows the same operations as the encoder MP-GNN.

The output of the MP-GNN is the furniture subgraph  $G_F^L$  of the final graph  $G^L$ . Each furniture node of  $G^L$  is then individually processed through a MLP to produce parameters for the furniture layout graph distribution  $p_{\theta'}(G_F | Z, n_F, G_R, T)$ , which can be factorized in the following way:

$$p_{\theta'}(G_F | Z, n_F, G_R, T) = \prod_{i=1}^{n_F} p_{\theta'}(\text{shape}_i | Z, G_R, T) p_{\theta'}(\text{orien}_i | Z, G_R, T) p_{\theta'}(\text{loc}_i | Z, G_R, T) p_{\theta'}(\text{size}_i | \text{shape}_i) p_{\theta'}(\text{cat}_i | \text{shape}_i). \quad (4)$$

More specifically, we assume that given latent  $Z$ , room layout  $G_R$  and type  $T$ , the furniture features are independent of each other (a standard assumption in the VAE literature). For a furniture, we further assume that shape, orientation and location features are independent given  $Z, G_F$  and  $T$ . However, since the PointNet shape features implicitly capture the configuration of the furniture item in 3D space we condition the size and category distributions on the shape feature.

We parameterize the shape and location features as a normal distribution, the size feature as a lognormal distribution whose support is restricted to be positive valued, category and orientation features as categorical distributions. Since both the Encoder and Decoder graphs have  $n_F$  nodes that are in one-to-one correspondence, we can define our reconstruction loss (first term in (3)) by simply comparing there node features without the need for an explicit matching procedure.

**Graph Prior.** Recall our latent space  $Z$  is modelled such that there is a latent variable corresponding to each furniture node in the graph. Many popular graph VAE models assume an i.i.d. normal prior for each node Kipf und Welling (2016b); Luo u. a. (2020). However, such a model is restrictive for our purposes. MP-GNNs achieve permutation equivariance by sharing the weight matrices across every node in the graph. When the graph is complete, as is the case here, the marginal distribution of every output node after  $L$  GNN layers will be identical if they are initialized as i.i.d. Gaussian at the input layer. Since, the output nodes of the decoder GNN after  $L$  layers correspond to different furniture features, having identical marginals is detrimental. We support this claim with ablation studies (Sec. 4) where we show that i.i.d. prior models struggle to learn the dependencies between different furniture categories in a room.

To remedy this, we propose to parameterize prior distribution as an autoregressive model based on linear gaussian models Bishop (2006). More specifically,

$$p(Z^0 | G_R, T) = \mathcal{N}(\mu_{\theta''}(G_R, T), \sigma_{\theta''}^0(G_R, T)),$$

$$p(Z^i | Z^{k < i}, G_R, T) = \mathcal{N}(\sum_{k < i} A_{\theta''}^k(G_R, T) Z^k, \sigma_{\theta''}^i(G_R, T)). \quad (5)$$

where  $Z^i$  refers to the latent corresponding to the  $i^{th}$  furniture node. Thus, the  $i^{th}$  furniture node latent is given by a Gaussian whose mean is a linear function of all the latents  $k < i$ . Such a structure ensures that all the latent variables are jointly Gaussian. This allows us to analytically compute the KL divergence term and thus was favoured over more expressive probabilistic models which would introduce more stochasticity in the objective due to the need of estimating the KL divergence term via sampling. We implement (5) (see also Figure 1) with two networks:

- **Room Aggregator for  $p(Z^0 | G_R, T)$ :** The room aggregator is an MP-GNN with the same architecture as the Graph Encoder. except that the input to the network is just  $(G_R, T)$  with the

node and edge features initialized to  $X_R$  and  $X_{RF}$ , respectively. After  $L$  GNN layers, all the room node features are aggregated by a mean pooling operation to obtain a global representation of the room layout plan  $X_R^{agg}$ . This  $X_R^{agg}$  is then passed through an MLP to compute  $\mu_{\theta''}(G_R, T)$  and  $\sigma_{\theta''}^0(G_R, T)$ .

- **RNN Prior for  $p(Z^i | Z^{k < i}, G_R, T)$ :** We use a recurrent neural network to predict the matrix  $A_{\theta''}^k(G_R, T)$  and the variance  $\sigma_{\theta''}^i(G_R, T)$  at each node index. The RNN is initialized with  $X_R^{agg}$ . We need additional constraints on each  $A_{\theta''}^k(G_R, T)$  to prevent the dynamics model in (5) from diverging to infinity. This is typically done by controlling the spectral radius or its proxy, the spectral norm Lacy und Bernstein (2003), of the matrices  $\{A_{\theta''}^k(G_R, T) : k \in [1, 2, \dots, n_F]\}$ . Thus, the predicted matrix is taken to be  $\frac{A_{\theta''}^k(G_R, T)}{\|A_{\theta''}^k(G_R, T)\|_2}$ , where  $\|A\|_2$  is the spectral norm of some matrix  $A$ .

### 3.3 Computing the KL term via matching and constrained learning

Note that the proposed autoregressive prior could in principle be reexpressed as a more traditional i.i.d. Gaussian prior, which is then passed through an additional non-equivariant transformation layer that can be absorbed into the decoder. But a significant difference emerges in practice when facing the key challenge of incorporating this non-equivariant factor into subsequent model training, given that there is no longer a canonical ordering between the different nodes in a graph. When the proposed autoregressive prior formulation is adopted, such an ordering is only required to evaluate  $p_{\theta''}(Z | G_R, T, n_F)$  for any  $Z$  sampled from the posterior  $q_\phi(Z | G, T, n_F)$  to compute the KL divergence term in the ELBO (3). However, by design this term can be expressed analytically, and as we will soon demonstrate, an efficient compensatory permutation can be efficiently computed. In contrast, with an alternative autoregressive decoder formulation, the search for an appropriate ordering is instead needed for computing the VAE reconstruction term (i.e., evaluating the decoder  $p_{\theta'}(G_F | Z, n_F, G_R, T)$  for any  $Z$  sampled from the posterior), and hence becomes entangled with the non-analytic stochastic sampling required for obtaining approximate reconstructions.

**Computing the KL divergence term.** Let  $Z = \{Z^1, Z^2, \dots, Z^{n_F}\}$  be the set of latent variables corresponding to  $n_F$  furniture items to be placed in the room. Let  $\pi$  denote the ordering among these variables. Given  $\pi$ , the likelihood of observing  $Z$  under our proposed prior is defined as

$$p_{\theta''}(Z | G_R, \pi, n_F, T) = \prod_{i=1}^{n_F} p_{\theta''}(Z^{\pi(i)} | Z^{\pi(j < i)}, G_R, T), \quad (6)$$

However, for  $Z \sim q_\phi(Z | G, T, n_F)$  (the approximate posterior) we do not know this ordering  $\pi$ . Thus, given  $Z$ , we define the optimal order  $\pi^*$  to be

$$\pi^* = \arg \min_{\pi} KL(q_\phi(Z | G, T, n_F) || p_{\theta''}(Z | G_R, \pi, n_F, T)). \quad (7)$$

Recall  $q_\phi(Z | G, T, n_F) = \prod_{i=1}^{n_F} \mathcal{N}(Z^i; \mu_\phi^i(G), \sigma_\phi^i(G))$ . Since both the prior and posterior are jointly Gaussian, computing (7) reduces to solving a Quadratic Assignment Problem (QAP). For simplicity let us denote the distributions as

$$q_\phi(Z | G, T, n_F) = \mathcal{N}(\mu_0, \Sigma_0); \quad p_{\theta''}(Z | G_R, \pi, n_F, T) = \mathcal{N}(\tilde{\pi}\mu_1, \tilde{\pi}\Sigma_1\tilde{\pi}^T), \quad (8)$$

where  $\tilde{\pi} = \pi \otimes I_{d_F \times d_F}$ . Note  $\pi \in \mathbb{R}^{n_F \times n_F}$  and the kronecker product comes from the fact that we are only allowed to permute blocks of  $\mu_1$  and  $\Sigma_1$ , of size  $d_F$  and  $d_F \times d_F$  respectively, where  $d_F$  is the dimension of the latent variable used for each furniture node. In other words, we can only permute latent vectors corresponding to furniture nodes as a whole and not the intra dimensions of  $Z$  within any furniture node. Here  $\mu_0, \mu_1 \in \mathbb{R}^{n_F d_F}$ . Similarly,  $\Sigma_0, \Sigma_1 \in \mathbb{R}^{n_F d_F \times n_F d_F}$ . Note that due to the autoregressive structure  $\Sigma_1$  will not be a diagonal matrix.

We show in the appendix that (7) is equivalent to

$$\min_{\pi} Tr(\Sigma_1^{-1} \tilde{\pi}^T [\Sigma_0 + \mu_0 \mu_0^T] \tilde{\pi}) - 2Tr(\tilde{\pi}^T \mu_0 \mu_1^T \Sigma_1^{-1}). \quad (9)$$

Notice that (9) is a Quadratic Assignment Problem (QAP) which is known to be NP-Hard. For this we propose to use a fast approximation algorithm, called FAQ, introduced in Vogelstein u. a. (2015).

FAQ first relaxes the optimization problem from set of permutation matrices to the set of all doubly stochastic matrices. It then iteratively proceeds by solving linearizations of the objective (9) using the Franke-Wolfe method. These linearizations reduce the QAP to just a linear assignment problem (LAP), which can be efficiently solved by the Hungarian algorithm. After Franke-Wolfe terminates, we project the doubly stochastic solution back to the set of permutations by solving another LAP. FAQ has a runtime complexity that is cubic in the number of nodes per iteration which is faster than the quartic complexity of the matching procedure used in Simonovsky und Komodakis (2018). More details in Appendix.

We need to compute the optimal  $\pi^*$  for each graph in a mini-batch, and then compute the KL divergence term in (3) analytically given this ordering. We observe no significant gains in performance in running the FAQ algorithm more than 1 step per graph, which further speeds our method.

**Learning under constraints:** To facilitate faster convergence and also ensure fidelity of the learned solution, we enforce certain constraints on the reconstructed room. These constraints are derived from training data and do not require external annotations. Given input furniture graph  $G_F$  to the encoder and the reconstructed graph  $\tilde{G}_F$  by the decoder, we enforce the relative positions of predicted furnitures in  $\tilde{G}_F$  to be “close” to the ground truth relative positions in  $G_F$ . Similarly, we apply constraints on the relative position of the predicted furniture items with the room walls, windows and doors. Finally we apply a constraint penalizing the relative orientations between different furniture items from being too “far” away from the relative orientations in  $G$ . We explain these constraints more clearly in the Appendix.

Having described all the ingredients in our model, we finally present the complete optimization objective as

$$\max_{\theta', \theta'', \phi} \mathcal{L}(\theta', \theta'', \phi) \quad s.t. \quad \frac{1}{n} \sum_{i=1}^n \text{Constr}(G_i) \leq \epsilon. \quad (10)$$

Here  $\epsilon$  is a user-defined hyperparameter that determines the strictness of enforcing these constraints.  $\mathcal{L}(\theta', \theta'', \phi)$  is as defined in (2) and  $i$  is in iterator over the scene graphs in the training set. We employ the learning under constraints framework introduced by Chamon und Ribeiro (2020) which results in a primal-dual saddle point optimization problem. For completeness, we give exact algorithmic details in the Appendix.

### 3.4 Inference

For inference, we start with a room layout graph  $G_R$  and type  $T$  along with the number of furnitures to be placed in the room  $n_F$ . We then use the learnt autoregressive prior to sample  $n_F$  latent variables recursively. This latent  $Z$  along with  $(n_F, G_R, T)$  is processed by the graph decoder to generate the furniture layout subgraph  $G_F$ . For scene rendering, we use the predicted shape descriptor for each furniture item and perform a nearest neighbour lookup using the  $\ell_2$  distance against a database of 3D furniture mesh objects indexed by there respective PointNet feature. We then use the predicted size and orientation to place furnitures in the scene. Note the inclusion of shape descriptors allows the model to reason about different appearance of furniture items that is more room aware as opposed to retrieval based on just furniture category & size as in Wang u. a. (2020); Paschalidou u. a. (2021).

## 4 Experiments

In this section, we evaluate the effectiveness of the proposed approach qualitatively and quantitatively. More details and figures provided in the Appendix.

**Dataset:** We use the 3D-FRONT dataset Fu u. a. (2021) for all our experiments. The dataset consists of roughly 14k rooms, furnished with 3D mesh furniture items. We consider four room types, bedroom, living room, library, and dining room.

**Training Protocols:** All models were trained on a 80 : 20 train-test split. Since we use PointNet shape descriptors, we only predict 7 “super-categories” of furniture items<sup>2</sup>. Since furniture is mostly axis-aligned, we discretized the orientation into four categories [0, 90, 180, 270]. We also rotate

<sup>2</sup>Cabinet/Shelf, Bed, Chair, Table, Sofa, Pier/Stool, Lighting



Figure 2: *Qualitative comparison of our method with ATISS and baselines. Windows and doors and indicated by white rectangles*

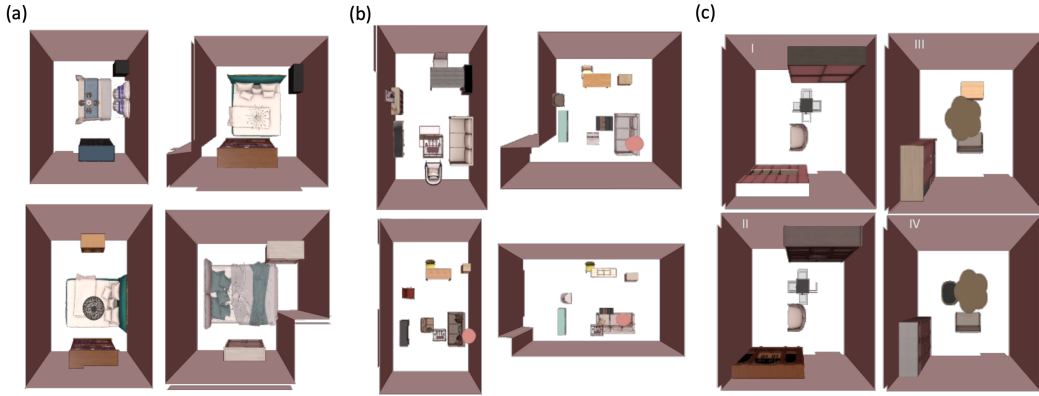


Figure 3: *Manipulating the latent space. (a), (b) recommendations made by our model for different rooms using the posterior distribution obtained from the reference room (first image in both figures); (c) by traversing the latent space one can “slightly” change the appearance and type of various furniture items*

the room by multiples of  $\frac{\pi}{2}$  degrees as data augmentations. We train all models using the ADAM optimizer for 1500 epochs with a batch size of 128. Each latent furniture is 64D.

**Baselines:** We compare our VAE model with baselines which have the same Encoder-Decoder architecture but employ the commonly used i.i.d. prior. We compare against two variants (inspired from Luo u. a. (2020)), (i) **Standard Prior (B1)**: Each  $Z^i \sim \mathcal{N}(0, I)$  for  $i \in [1, \dots, n_F]$ , (ii) **Non-autoregressive Learnt Prior (B2)**: Each  $Z^i \sim \mathcal{N}(\mu(G_R), \sigma(G_R))$ . The mean and variance parameters of this distribution are learnt by an MP-GNN which processes just the room subgraph.

**Scene Generation:** In Figure 1b, we illustrate the effectiveness of the proposed method at generating diverse furniture recommendations given a room layout. Notice how our model generates different furniture arrangements as well as diverse 3D appearances. For example, sampled beds, cabinets and ceiling lights look distinct in row 1. For the library example (row 2), our model proposes from a simple study room with a small shelf and seating (columns 2,3) to a lounge with a couch and a chair.

In Figure 2 we qualitatively compare our generations for different rooms with the state-of-the-art (ATISS) and our VAE baselines. Note that while both ATISS and our model generate plausible furniture arrangements the baseline VAEs struggle, presumably because of the i.i.d. prior assumption. Moreover, since ATISS does not explicitly model window and doors, often the furniture items occlude them which is undesirable (for example, cabinet partially blocking door in row 3 col 1). This is

Table 1: *Quantitative comparison of our method with other models and baselines. Scene classification accuracy closer to 0.5 is better*

	FID Score ( $\downarrow$ )				Category KL Divergence ( $\downarrow$ )				Scene Classification Accuracy			
	Bedroom	Living	Dining	Library	Bedroom	Living	Dining	Library	Bedroom	Living	Dining	Library
FastSynth	40.89	61.67	55.38	37.72	<b>0.01</b>	0.02	0.05	0.04	0.883	0.945	0.935	0.815
SceneFormer	43.17	69.54	67.04	55.45	<b>0.01</b>	0.03	0.03	0.02	0.945	0.972	0.941	0.880
ATISS	38.39	<b>33.14</b>	<b>29.23</b>	<b>35.24</b>	<b>0.01</b>	<b>0.00</b>	<b>0.01</b>	<b>0.01</b>	<b>0.562</b>	<b>0.516</b>	<b>0.477</b>	<b>0.521</b>
Baseline B1	56.82	39.47	63.56	76.87	0.02	0.02	0.05	0.09	0.953	0.912	0.757	0.864
Baseline B2	47.47	39.78	42.34	67.28	0.02	0.02	0.05	0.07	0.945	0.909	0.716	0.739
Ours	<b>34.86</b>	38.19	38.03	65.05	<b>0.01</b>	0.01	0.02	0.02	0.877	0.867	0.693	0.729

not the case in our method which explicitly accounts for windows and doors as nodes of the room sub-graph.

In Table 1, we provide competitive results compared to existing methods using the same experimental protocols in Paschalidou et al. (2021). FID score (lower is better), which measures the realism of generated indoor scenes v/s ground truth scenes from the test set. Our method performs the best on this metric for bedrooms and is comparable for living rooms and dining rooms. However, presumably due to fewer training data points, our network struggles on libraries. The Category KL divergence measures how well the model captures the frequency of categories present in an indoor scene compared to the ground truth. On this metric, our method is comparable to existing methods. Moreover, this metric can be misleading since it does not capture the dependencies between different predicted furniture items as we show in ablation studies. Scene classification accuracy (close to 0.5 is better) tests the ability of a network to distinguish between real and synthetic scenes. On this metric, our method performs better than both FastSynth and Sceneformer in all room types. Note that although ATISS appears quantitatively better at scene generation, it is autoregressive and thus does not share the benefits of latent-variable manipulations which we will discuss next.

**Manipulating the Latent space.** Suppose we are moving to a new apartment and would like to interior design our new place in the same “style” as the old apartment. How might we do this? This is a non-trivial problem since one needs to account for differences in room dimensions and size. Answering such questions is easier using latent-variable models where the latent  $Z$  is expected to capture the room design and can be easily manipulated. More concretely, given a “reference” furnished room graph. We can process it using our graph encoder to obtain the posterior distribution  $q(Z | G, T, n_F)$ . We can then use the room layout of our new apartment  $\tilde{G}_R$ , pass it through the decoder along with the latent  $Z \sim q(Z | G, T, n_F)$  to recommend furniture items for  $\tilde{G}_R$ . Figure 3a & b show two such examples. In both figures, the first image is the reference scene  $G$ . Notice how, according to the room layout, the bed or the sofa changes its orientation while the network tries to keep the overall arrangement the same. This shows that our model does not trivially memorize the furniture layout of the reference room in  $Z$  but uses the room structure  $\tilde{G}_R$  in making its predictions. *Such latent space manipulations are not possible in our baseline models, where the learnt GNN encoder simply memorizes each furniture pose in its latent and the decoder subsequently ignores the room structure in its generation.* This is validated by experiments in which we keep  $Z$  fixed and vary the room layout input to the GNN decoder. For the proposed model, the predicted furniture positions vary on average by 36 cms because of the room, whereas for our baseline VAEs the furniture predicted positions vary on average by only 10 cms.

Further, we show in Figure 3c that our model learns a smooth latent space which could be exploited to change the “style” of the recommendations. To do this, we sample two latents  $Z_1$  and  $Z_2$  from the prior for the same room layout. We then interpolate along a straight line from  $Z_1$  to  $Z_2$  and visualize the corresponding furniture recommendations made by the GNN decoder, we observe a smooth transition from a room with two cabinets, a chair, and a light (No. I) to a room with a aesthetically different chair, table & cabinet (No. IV).

**Ablation studies.** We showed that our model performs better than baseline VAEs both qualitatively (Figure 2) and quantitatively (Table 1). We now show in Figure 4, that the proposed autoregressive prior better captures the co-occurrence structure between categories than our baselines. Notice that for both baselines, beds are synthesized in all room types, whereas our model correctly learns that beds must be present only in bedrooms. We also analyzed matched furniture nodes for the trained model, that is, the solution to (7). We found that the first bedroom item matched by our model is a nightstand/bed/light with probability 0.91 and the first living room item matched is a

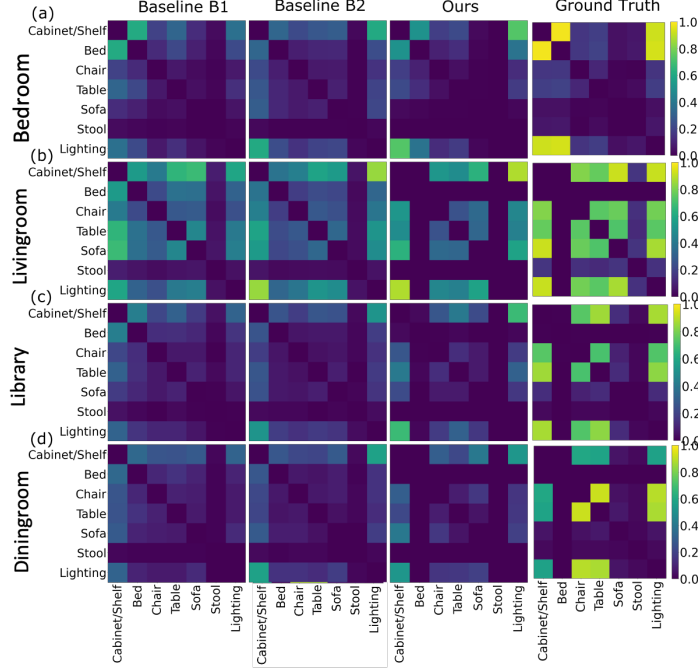


Figure 4: Co-occurrence heatmaps show the pairwise distribution of different furniture categories. Rows are arranged according to room type, while columns depict the co-occurrence statistics for scenes synthesized using the indicated method. Cell  $ij$  in each heatmap represents the probability that furniture category  $i$  and  $j$  will co-occur in the same scene

coffee-table/sofa/light with probability 0.76. This is interesting since human designers often start planning with these items.

## 5 Limitations and Conclusion

We have presented a latent-variable model for generating 3D indoor scenes given the room type and layout. While we show our model’s ability to generate diverse scenes, it still lags behind purely autoregressive models in terms of quantitative metrics. It would be interesting to see if this gap can be closed using more expressive non-linear autoregressive priors; however the KL divergence cannot be computed analytically and the subsequent matching will not be quadratic. Moreover, the matching procedure introduced in this paper for training VAEs is novel and can be potentially useful in other permutation-invariant domains like sets.

## References

- [Armeni u. a. 2019] ARMENI, Iro ; HE, Zhi-Yang ; GWAK, JunYoung ; ZAMIR, Amir R. ; FISCHER, Martin ; MALIK, Jitendra ; SAVARESE, Silvio: 3D Scene Graph: A Structure for Unified Semantics, 3D Space, and Camera. In: *IEEE/CVF International Conference on Computer Vision*, 2019, S. 5664–5673
- [Bishop 2006] BISHOP, Christopher M.: Pattern recognition. In: *Machine learning* 128 (2006), Nr. 9
- [Chamon und Ribeiro 2020] CHAMON, Luiz ; RIBEIRO, Alejandro: Probably approximately correct constrained learning. In: *Advances in Neural Information Processing Systems* 33 (2020)
- [Chang u. a. 2015] CHANG, Angel X. ; FUNKHOUSER, Thomas ; GUIBAS, Leonidas ; HANRAHAN, Pat ; HUANG, Qixing ; LI, Zimo ; SAVARESE, Silvio ; SAVVA, Manolis ; SONG, Shuran ; SU, Hao ; XIAO, Jianxiong ; YI, Li ; YU, Fisher: ShapeNet: An Information-Rich 3D Model Repository / Stanford University — Princeton University — Toyota Technological Institute at Chicago. 2015 (arXiv:1512.03012 [cs.GR]). — Forschungsbericht

- [Chen u. a. 2016] CHEN, Xi ; KINGMA, Diederik P. ; SALIMANS, Tim ; DUAN, Yan ; DHARIWAL, Prafulla ; SCHULMAN, John ; SUTSKEVER, Ilya ; ABBEEL, Pieter: Variational lossy autoencoder. In: *arXiv preprint arXiv:1611.02731* (2016)
- [Fisher u. a. 2012] FISHER, Matthew ; RITCHIE, Daniel ; SAVVA, Manolis ; FUNKHOUSER, Thomas ; HANRAHAN, Pat: Example-based synthesis of 3D object arrangements. In: *ACM Transactions on Graphics (TOG)* 31 (2012), Nr. 6, S. 1–11
- [Fisher u. a. 2011] FISHER, Matthew ; SAVVA, Manolis ; HANRAHAN, Pat: Characterizing structural relationships in scenes using graph kernels. In: *ACM SIGGRAPH 2011 papers*. 2011, S. 1–12
- [Fu u. a. 2021] FU, Huan ; CAI, Bowen ; GAO, Lin ; ZHANG, Ling-Xiao ; WANG, Jiaming ; LI, Cao ; ZENG, Qixun ; SUN, Chengyue ; JIA, Rongfei ; ZHAO, Binqiang u. a.: 3d-front: 3d furnished rooms with layouts and semantics. In: *Proceedings of the IEEE/CVF International Conference on Computer Vision*, 2021, S. 10933–10942
- [Gadde u. a. 2021] GADDE, Raghudeep ; FENG, Qianli ; MARTINEZ, Aleix M.: Detail Me More: Improving GAN’s Photo-Realism of Complex Scenes. In: *Proceedings of the IEEE/CVF International Conference on Computer Vision (ICCV)*, October 2021, S. 13950–13959
- [Goodfellow u. a. 2014] GOODFELLOW, Ian ; POUGET-ABADIE, Jean ; MIRZA, Mehdi ; XU, Bing ; WARDE-FARLEY, David ; OZAIR, Sherjil ; COURVILLE, Aaron ; BENGIO, Yoshua: Generative Adversarial Nets. In: GHAHRAMANI, Z. (Hrsg.) ; WELLING, M. (Hrsg.) ; CORTES, C. (Hrsg.) ; LAWRENCE, N. (Hrsg.) ; WEINBERGER, K. Q. (Hrsg.): *Advances in Neural Information Processing Systems* Bd. 27, Curran Associates, Inc., 2014. – URL <https://proceedings.neurips.cc/paper/2014/file/5ca3e9b122f61f8f06494c97b1afccf3-Paper.pdf>
- [Higgins u. a. 2016] HIGGINS, Irina ; MATTHEY, Loic ; PAL, Arka ; BURGESS, Christopher ; GLOROT, Xavier ; BOTVINICK, Matthew ; MOHAMED, Shakir ; LERCHNER, Alexander: beta-vae: Learning basic visual concepts with a constrained variational framework. (2016)
- [Jiang u. a. 2018] JIANG, Chenfanfu ; QI, Siyuan ; ZHU, Yixin ; HUANG, Siyuan ; LIN, Jenny ; YU, Lap-Fai ; TERZOPOULOS, Demetri ; ZHU, Song-Chun: Configurable 3d scene synthesis and 2d image rendering with per-pixel ground truth using stochastic grammars. In: *International Journal of Computer Vision* 126 (2018), Nr. 9, S. 920–941
- [Karras u. a. 2020] KARRAS, Tero ; LAINE, Samuli ; AITTALA, Miika ; HELLSTEN, Janne ; LEHTINEN, Jaakko ; AILA, Timo: Analyzing and Improving the Image Quality of StyleGAN. In: *Proceedings of the IEEE/CVF Conference on Computer Vision and Pattern Recognition (CVPR)*, June 2020
- [Keshavarzi u. a. 2020] KESHAVARZI, Mohammad ; PARIKH, Aakash ; ZHAI, Xiyu ; MAO, Melody ; CALDAS, Luisa ; YANG, Allen: Scenegen: Generative contextual scene augmentation using scene graph priors. In: *arXiv preprint arXiv:2009.12395* (2020)
- [Kingma u. a. 2014] KINGMA, Diederik P. ; MOHAMED, Shakir ; REZENDE, Danilo J. ; WELLING, Max: Semi-supervised learning with deep generative models. In: *Advances in neural information processing systems*, 2014, S. 3581–3589
- [Kingma und Welling 2014] KINGMA, Diederik P. ; WELLING, Max: Auto-Encoding Variational Bayes. In: *CoRR* abs/1312.6114 (2014)
- [Kipf und Welling 2016a] KIPF, Thomas ; WELLING, Max: Variational Graph Auto-Encoders. In: *ArXiv abs/1611.07308* (2016)
- [Kipf und Welling 2016b] KIPF, Thomas N. ; WELLING, Max: Variational graph auto-encoders. In: *arXiv preprint arXiv:1611.07308* (2016)
- [Klushyn u. a. 2019] KLUSHYN, Alexej ; CHEN, Nutan ; KURLE, Richard ; CSEKE, Botond ; SMAGT, Patrick van der: Learning hierarchical priors in vaes. In: *arXiv preprint arXiv:1905.04982* (2019)
- [Kumar u. a. 2017] KUMAR, Abhishek ; SATTIGERI, Prasanna ; BALAKRISHNAN, Avinash: Variational inference of disentangled latent concepts from unlabeled observations. In: *arXiv preprint arXiv:1711.00848* (2017)
- [Kusner u. a. 2017] KUSNER, Matt J. ; PAIGE, Brooks ; HERNÁNDEZ-LOBATO, José M.: Grammar variational autoencoder. In: *International Conference on Machine Learning PMLR* (Veranst.), 2017, S. 1945–1954



- [Lacy und Bernstein 2003] LACY, Seth L. ; BERNSTEIN, Dennis S.: Subspace identification with guaranteed stability using constrained optimization. In: *IEEE Transactions on automatic control* 48 (2003), Nr. 7, S. 1259–1263
- [Li u. a. 2019] LI, Manyi ; PATIL, Akshay G. ; XU, Kai ; CHAUDHURI, Siddhartha ; KHAN, Owais ; SHAMIR, Ariel ; TU, Changhe ; CHEN, Baoquan ; COHEN-OR, Daniel ; ZHANG, Hao: Grains: Generative recursive autoencoders for indoor scenes. In: *ACM Transactions on Graphics (TOG)* 38 (2019), Nr. 2, S. 1–16
- [Luo u. a. 2020] LUO, Andrew ; ZHANG, Zhoutong ; WU, Jiajun ; TENENBAUM, Joshua B.: End-to-End Optimization of Scene Layout. In: *Proceedings of the IEEE/CVF Conference on Computer Vision and Pattern Recognition*, 2020, S. 3754–3763
- [Mavroudi u. a. 2020] MAVROUDI, Effrosyni ; HARO, Benjamín Béjar ; VIDAL, René: Representation learning on visual-symbolic graphs for video understanding. In: *European Conference on Computer Vision* Springer (Veranst.), 2020, S. 71–90
- [Para u. a. 2021] PARA, Wamiq ; GUERRERO, Paul ; KELLY, Tom ; GUIBAS, Leonidas J. ; WONKA, Peter: Generative layout modeling using constraint graphs. In: *Proceedings of the IEEE/CVF International Conference on Computer Vision*, 2021, S. 6690–6700
- [Paschalidou u. a. 2021] PASCHALIDOU, Despoina ; KAR, Amlan ; SHUGRINA, Maria ; KREIS, Karsten ; GEIGER, Andreas ; FIDLER, Sanja: ATISS: Autoregressive Transformers for Indoor Scene Synthesis. In: *Advances in Neural Information Processing Systems (NeurIPS)*, 2021
- [Purkait u. a. 2020] PURKAIT, Pulak ; ZACH, Christopher ; REID, Ian: SG-VAE: Scene Grammar Variational Autoencoder to generate new indoor scenes. In: *European Conference on Computer Vision* Springer (Veranst.), 2020, S. 155–171
- [Qi u. a. 2017] QI, Charles R. ; SU, Hao ; MO, Kaichun ; GUIBAS, Leonidas J.: Pointnet: Deep learning on point sets for 3d classification and segmentation. In: *Proceedings of the IEEE conference on computer vision and pattern recognition*, 2017, S. 652–660
- [Qi u. a. 2018] QI, Siyuan ; ZHU, Yixin ; HUANG, Siyuan ; JIANG, Chenfanfu ; ZHU, Song-Chun: Human-centric indoor scene synthesis using stochastic grammar. In: *Proceedings of the IEEE Conference on Computer Vision and Pattern Recognition*, 2018, S. 5899–5908
- [Rezende und Mohamed 2015] REZENDE, Danilo ; MOHAMED, Shakir: Variational inference with normalizing flows. In: *International conference on machine learning* PMLR (Veranst.), 2015, S. 1530–1538
- [Ritchie u. a. 2019] RITCHIE, Daniel ; WANG, Kai ; LIN, Yu-An: Fast and Flexible Indoor Scene Synthesis via Deep Convolutional Generative Models. In: *IEEE/CVF Conference on Computer Vision and Pattern Recognition (CVPR)*, 2019, S. 6175–6183
- [Simonovsky und Komodakis 2018] SIMONOVSKY, Martin ; KOMODAKIS, Nikos: Graphvae: Towards generation of small graphs using variational autoencoders. In: *International conference on artificial neural networks* Springer (Veranst.), 2018, S. 412–422
- [Tomczak und Welling 2018] TOMCZAK, Jakub ; WELLING, Max: VAE with a VampPrior. In: *International Conference on Artificial Intelligence and Statistics* PMLR (Veranst.), 2018, S. 1214–1223
- [Vaswani u. a. 2017] VASWANI, Ashish ; SHAZEER, Noam ; PARMAR, Niki ; USZKOREIT, Jakob ; JONES, Llion ; GOMEZ, Aidan N. ; KAISER, Ł u. ; POLOSUKHIN, Illia: Attention is All you Need. In: GUYON, I. (Hrsg.) ; LUXBURG, U. V. (Hrsg.) ; BENGIO, S. (Hrsg.) ; WALLACH, H. (Hrsg.) ; FERGUS, R. (Hrsg.) ; VISHWANATHAN, S. (Hrsg.) ; GARNETT, R. (Hrsg.): *Advances in Neural Information Processing Systems* Bd. 30, Curran Associates, Inc., 2017. – URL <https://proceedings.neurips.cc/paper/2017/file/3f5ee243547dee91fbd053c1c4a845aa-Paper.pdf>
- [Vogelstein u. a. 2015] VOGELSTEIN, Joshua T. ; CONROY, John M. ; LYZINSKI, Vince ; PODRAZIK, Louis J. ; KRATZER, Steven G. ; HARLEY, Eric T. ; FISHKIND, Donniell E. ; VOGELSTEIN, R J. ; PRIEBE, Carey E.: Fast approximate quadratic programming for graph matching. In: *PLOS one* 10 (2015), Nr. 4, S. e0121002
- [Wang u. a. 2019] WANG, Kai ; LIN, Yu-An ; WEISSMANN, Ben ; SAVVA, Manolis ; CHANG, Angel X. ; RITCHIE, Daniel: Planit: Planning and instantiating indoor scenes with relation graph and spatial prior networks. In: *ACM Transactions on Graphics (TOG)* 38 (2019), Nr. 4, S. 1–15
- [Wang u. a. 2018] WANG, Kai ; SAVVA, Manolis ; CHANG, Angel X. ; RITCHIE, Daniel: Deep convolutional priors for indoor scene synthesis. In: *ACM Transactions on Graphics (TOG)* 37 (2018), Nr. 4, S. 1–14

- [Wang u. a. 2020] WANG, Xinpeng ; YESHWANTH, Chandan ; NIESSNER, Matthias: Sceneformer: Indoor scene generation with transformers. In: *arXiv preprint arXiv:2012.09793* (2020)
- [Yeh u. a. 2012] YEH, Yi-Ting ; YANG, Lingfeng ; WATSON, Matthew ; GOODMAN, Noah D. ; HANRAHAN, Pat: Synthesizing open worlds with constraints using locally annealed reversible jump mcmc. In: *ACM Transactions on Graphics (TOG)* 31 (2012), Nr. 4, S. 1–11
- [Zhang u. a. 2020] ZHANG, Zaiwei ; YANG, Zhenpei ; MA, Chongyang ; LUO, Linjie ; HUTH, Alexander ; VOUGA, Etienne ; HUANG, Qixing: Deep generative modeling for scene synthesis via hybrid representations. In: *ACM Transactions on Graphics (TOG)* 39 (2020), Nr. 2, S. 1–21

## 6 Appendix

### 6.1 Feature engineering

As explained in Section 3.1, our indoor scene representation is an attributed graph. We now describe these attributes in detail.

- **Room node features  $X_R$ ,**
  1. **Node Type:** A 4D 1-hot embedding of the node type. The four categories are wall, door, floor, window.
  2. **Room Type:** A 4D 1-hot embedding of the room type. The four categories are living room, bedroom, dining room, library.
  3. **Location:** A 6D vector representing the minimum and maximum vertex positions of the 3D bounding box corresponding to the room node.
  4. **Normal:** A 3D vector representing the direction of the normal vector corresponding to the room node.
- **Furniture node features  $X_F$ ,**
  1. **Super category:** A 7D 1-hot embedding of the node type. The seven categories are Cabinet/Shelf, Bed, Chair, Table, Sofa, Pier/Stool, Lighting.
  2. **Shape:** A 1024D embedding of the 3D shape descriptor obtained by processing a 3D point cloud of the furniture item through PointNet.
  3. **Location:** A 3D vector representing the centroid of the furniture item.
  4. **Orientation:** A 3D vector representing the direction the “front” side of the furniture is facing.
  5. **Size:** A 3D vector representing the dimensions of the furniture along each axis.
- **Furniture-furniture edge features  $X_{FF}$ ,** let us arbitrarily chose a furniture-furniture edge and label its source node as  $s$  with receiver node as  $r$ . We will describe the features for this edge.
  1. **Center-center distance:** A scalar representing the distance between the centroids of furniture  $s$  and  $r$ .
  2. **Relative orientation:** A scalar representing the signed dot product between the orientation feature of  $s$  and  $r$ .
  3. **Center-center orientation:** A 3D vector representing the unit vector connecting the centroids of  $r$  and  $s$ .
  4. **Orientation:** A 3D vector representing the direction the “front” side of the furniture is facing.
  5. **Bbox-bbox distance:** The shortest distance between the corners of the bounding box of  $s$  and  $r$ .
- **Room-furniture edge features  $X_{RF}$ ,** let us arbitrarily chose a room-furniture edge and label its source node as  $s$  with receiver node as  $r$ . We will describe the features for this edge.
  1. **Center-room distance:** A scalar representing the distance between the centroid of furniture  $r$  and room node  $s$ . This is computed in 2D as a point to line distance. Every wall/window/door can be treated as a line segment in 2D.
  2. **Center-room center:** A scalar representing the distance between the centroids of  $r$  and  $s$ .
  3. **Bbox-room dist** A scalar representing the shortest distance between corners of the bounding box of furniture item  $r$  to the room node  $s$ . This is computed in 2D as a point-to-line distance.
  4. **Bbox-room center** A scalar representing the shortest distance between corners of the bounding box of furniture item  $r$  to the centroid of the room node  $s$ .
  5. **Relative orientation:** A signed dot product between the normal of  $s$  with the orientation attribute of  $r$ .

- **Room-room edge features  $X_{RR}$** , let us arbitrarily chose a room-room edge and label its source node as  $s$  with receiver node as  $r$ . We will describe the features for this edge.
  1. **Center-center distance:** A scalar representing the distance between the centroids of room nodes  $s$  and  $r$ .
  2. **Relative orientation:** A scalar representing the signed dot product between the normal vectors of  $s$  and  $r$ .
  3. **Longest distance:** A scalar representing the longest distance between the corners of the bounding boxes of  $r$  and  $s$ .
  4. **Shortest distance:** A scalar representing the shortest distance between the corners of the bounding boxes of  $r$  and  $s$ .

## 6.2 Architecture Details

### 6.2.1 Message-Passing Graph Neural Network (MP-GNN)

Here we describe the message-passing mechanism employed in the Graph Neural Networks used in this work. The design of the MP-GNN is inspired by the work of Mavroudi u. a. (2020), where each layer  $l = 1, \dots, L$  of the MP-GNN maps a graph  $G^{l-1}$  to another graph  $G^l$  by updating the graph's node and edge features. Specifically, let  $h_i^l$  and  $h_{ij}^l$  denote the features of node  $i$  and edge  $(i, j)$  of graph  $G^l$ , respectively. Let the input to the network be the graph  $G^0 = G$ , so that  $h_i^0$  and  $h_{ij}^0$  denote the node features and edge features, respectively. At each iteration of node and edge refinement, the MP-GNN: (1) adapts the scalar edge weights by using an attention mechanism; (2) updates the edge attributes depending on the edge type, the attention-based edge weights, the attributes of the connected nodes and the previous edge attribute; and (3) updates the node attribute by aggregating attributes from incoming edges, as described next.

*Computing attention coefficients:* At each step  $l$  of refinement, we update the scalar edge weights by computing an attention coefficient  $a_{ij}^l$  that measures the relevance of node  $j$  for node  $i$  as follows:

$$\begin{aligned} \gamma_{ij}^l &= \rho(w_a^{\epsilon_{ij}} \top [W_r^{\nu_i} h_i^l; W_s^{\nu_j} h_j^l; W_{rs}^{\epsilon_{ij}} h_{ij}^l]) \\ a_{ij}^l &= \frac{\exp(\gamma_{ij}^l)}{\sum_{k \in N_{\epsilon_{ij}}(i)} \exp(\gamma_{ik}^l)}, \quad \forall (i, j) \in E. \end{aligned} \quad (11)$$

In the first equation, each edge  $(i, j)$  of  $G_l = (V, E, X_l)$  is associated with a score,  $\gamma_{ij}^l$ , obtained by applying a nonlinearity  $\rho$  (e.g., a leaky ReLU) to the dot product between a vector of attention weights  $w_a^{\epsilon_{ij}}$  for edge type  $\epsilon_{ij} \in \{RR, RF, FF\}$ , and the concatenation of five vectors: (1) the receiver node feature  $h_i^l \in \mathbb{R}^{d_i}$  weighted by a matrix  $W_r^{\nu_i}$  for node type  $\nu_i \in \{R, F\}$ , (2) the sender node feature  $h_j^l$  weighted by a matrix  $W_s^{\nu_j}$  for node type  $\nu_j$ , and (3) the receiver-sender edge feature  $h_{ij}^l$  weighted by a matrix  $W_{rs}^{\epsilon_{ij}}$  for edge type  $\epsilon_{ij}$ . All weight matrices are also indexed by the GNN layer  $l$  which is suppressed to prevent notational clutter.

*Updating the node and edge features:* At each step  $l$  of refinement, we update the edge and node features as:

$$\begin{aligned} h_{ij}^l &= a_{ij}^l (U_{edge}^{\epsilon_{ij}} W_s^{\nu_j} h_j^{l-1} + W_{rs}^{\epsilon_{ij}} h_{ij}^{l-1}), \quad \forall (i, j) \in E \\ h_i^l &= \rho(h_i^{l-1} + \sum_{k \in N_{\epsilon_{ij}}(i)} U_{node}^{\epsilon_{ij}} W_s h_{ik}^l), \quad \forall i \in V. \end{aligned} \quad (12)$$

The first equation updates the features of edge  $(i, j)$  by taking a weighted combination of the features of node  $j$  and the features of edge  $(i, j)$  in the previous layer, with weight matrices  $W_s^{\nu_j}$  and  $W_{rs}^{\epsilon_{ij}}$ , respectively. The matrix  $U_{edge}^{\epsilon_{ij}}$  is a learnable projection matrix to change the dimensionality of the first term (transformed node feature) with that of the second term (transformed edge feature).

The second equation updates the feature of node  $i$  as the sum of the feature of node  $i$  from the previous layer (a residual connection) and the sum of the features of all edges connected to node  $i$  after applying a non-linearity  $\rho$ , such as a ReLU or leaky-ReLU. Here,  $U_{node}^{\epsilon_{ij}}$  denotes a learnable projection matrix for edge type  $\epsilon_{ij}$ .

All weight matrices are also indexed by the GNN layer  $l$  which is suppressed to prevent notational clutter.

Table 2: Encoder architecture. The network parameters are as defined in Section 6.2.1

Encoder			
Network parameters	Layer 1	Layer 2	Layer 3
$W_{r/s}^R$	17×17	17×17	17×17
$W_{r/s}^F$	256×1034	128×256	64×128
$W_{rs}^{FF}$	26×6	52×26	6×52
$W_{rs}^{RR}$	26×4	52×26	6×52
$W_{rs}^{RF}$	26×5	52×26	6×52
$w_a^{FF}$	1×538	1×308	1×134
$w_a^{RR}$	1×60	1×86	1×40
$w_a^{RF}$	1×299	1×197	1×87
$U_{edge}^{FF}$	26×256	52×128	6×64
$U_{edge}^{RR}$	26×17	52×17	6×17
$U_{edge}^{RF}$	26×17	52×17	6×17
$U_{node}^{FF}$	256×26	128×52	64×6
$U_{node}^{RR}$	17×26	17×52	17×6
$U_{node}^{RF}$	256×26	128×52	64×6

### 6.2.2 Encoder, Decoder and Room Aggregator networks

We employ three MP-GNNs in this work. One for the VAE encoder, one for the decoder and one for the Room Aggregator component of the prior network. Each of these MP-GNNs are three layered graph neural networks. In Table 2, 3, 4 we summarize the architecture of the Encoder, Decoder and Room Aggregator networks respectively.

The RNN Prior network (second component of our Graph Prior) is implemented by a single layer Gated Recurrent Unit (GRU) with hidden vector of size  $64 \times 64$  (the latent space is 64D).

### 6.3 The Reconstruction Loss of the ELBO

The reconstruction loss is the first term in the ELBO (3).

$$\mathbb{E}_{Z \sim q_\phi(Z|G,T,n_F)}[\log p_{\theta'}(G_F | Z, n_F, G_R, T)]$$

In subsection 3.2 we described the distribution  $p_{\theta'}(G_F | Z, n_F, G_R, T)$  as

$$\begin{aligned} & p_{\theta'}(G_F | Z, n_F, G_R, T) \\ &= \prod_{i=1}^{n_F} p_{\theta'}(shape_i | Z, G_R, T) p_{\theta'}(orien_i | Z, G_R, T) \\ & \quad p_{\theta'}(loc_i | Z, G_R, T) p_{\theta'}(size_i | shape_i) p_{\theta'}(cat_i | shape_i). \end{aligned}$$

Here  $shape_i$ ,  $orien_i$ ,  $loc_i$ ,  $size_i$  and  $cat_i$  refer to the ground truth values of the 3D shape descriptor (PointNet features), orientation, location, size and category respectively for furniture node  $i$  in  $G_F$ .

We will now describe each of these distributions in detail along with the corresponding loss term. For the normal and lognormal distributions used we assume the variance parameter is a fixed constant equal to 1 and do not learn them.

Table 3: Decoder architecture. The network parameters are as defined in Section 6.2.1

Decoder			
Network parameters	Layer 1	Layer 2	Layer 3
$W_{r/s}^R$	17×17	17×17	17×17
$W_{r/s}^F$	128×64	256×128	1034×256
$W_{rs}^{FF}$	26×128	52×26	6×52
$W_{rs}^{RR}$	26×4	52×26	6×52
$W_{rs}^{RF}$	26×81	52×26	6×52
$w_a^{FF}$	1×282	1×564	1×2074
$w_a^{RR}$	1×60	1×86	1×40
$w_a^{RF}$	1×171	1×325	1×1057
$U_{edge}^{FF}$	26×128	52×256	6×1034
$U_{edge}^{RR}$	26×17	52×17	6×17
$U_{edge}^{RF}$	26×17	52×17	6×17
$U_{node}^{FF}$	128×26	256×52	1034×6
$U_{node}^{RR}$	17×26	17×52	17×6
$U_{node}^{RF}$	128×26	256×52	1034×6

Table 4: Room Aggregator architecture. This network only processes the room subgraph  $G_R$  and hence all the weight matrices associated with furniture nodes are absent. The network parameters are as defined in Section 6.2.1

Room Aggregator			
Network parameters	Layer 1	Layer 2	Layer 3
$W_{r/s}^R$	32×17	48×32	64×48
$W_{rs}^{RR}$	26×4	52×26	6×52
$w_a^{RR}$	1×90	1×148	1×134
$U_{edge}^{RR}$	26×32	52×48	6×64
$U_{node}^{RR}$	32×26	48×52	64×6

$$\begin{aligned}
p_{\theta'}(\text{shape}_i \mid Z, G_R, T) &= \mathcal{N}(\mu_{\theta'}^{\text{shape}}(Z, G_R, T), \text{const.}) \\
\log p_{\theta'}(\text{shape}_i \mid Z, G_R, T) &= - \left( \mu_{\theta'}^{\text{shape}}(Z, G_R, T) - \text{shape}_i \right)^2 \\
p_{\theta'}(\text{orient}_i \mid Z, G_R, T) &= \text{Categorical}(\Theta_{\theta'}^{\text{orient}}(Z, G_R, T)) \\
\log p_{\theta'}(\text{orient}_i \mid Z, G_R, T) &= -H(\text{orient}_i, \Theta_{\theta'}^{\text{orient}}(Z, G_R, T))
\end{aligned}$$

$\text{orient}_i$  is a 4D 1-hot embedding of the ground truth orientation and  $\Theta$  is the parameter of the categorical distribution.  $H(., .)$  denotes the cross entropy between two distributions.

$$\begin{aligned}
p_{\theta'}(\text{loc}_i \mid Z, G_R, T) &= \mathcal{N}(\mu_{\theta'}^{\text{loc}}(Z, G_R, T), \text{const.}) \\
\log p_{\theta'}(\text{loc}_i \mid Z, G_R, T) &= - \left( \mu_{\theta'}^{\text{loc}}(Z, G_R, T) - \text{loc}_i \right)^2 \\
p_{\theta'}(\text{size}_i \mid \text{shape}_i) &= \\
&\quad \text{LogNormal}(\mu_{\theta'}^{\text{size}}(\mu_{\theta'}^{\text{shape}}(Z, G_R, T)), \text{const.}) \\
\log p_{\theta'}(\text{size}_i \mid \text{shape}_i) &= \\
&\quad - \left( \mu_{\theta'}^{\text{size}}(\mu_{\theta'}^{\text{shape}}(Z, G_R, T)) - \ln \text{size}_i \right)^2 \\
p_{\theta'}(\text{cat}_i \mid \text{shape}_i) &= \text{Categorical}(\Theta_{\theta'}^{\text{cat}}(\mu_{\theta'}^{\text{shape}}(Z, G_R, T))) \\
\log p_{\theta'}(\text{cat}_i \mid \text{shape}_i) &= -H(\text{cat}_i, \Theta_{\theta'}^{\text{cat}}(\mu_{\theta'}^{\text{shape}}(Z, G_R, T)))
\end{aligned}$$

Each furniture node feature in the output of the MP-GNN Decoder is individually processed using a multi-layer Perceptron (MLP). Specifically, let  $\hat{h}_i^L$  be the output feature of the decoder for furniture node  $i$ . In our experiments  $\hat{h}_i^L \in \mathbb{R}^{1034}$ .

$$\begin{aligned}
\mu_{\theta'}^{\text{shape}}(Z, G_R, T) &= \text{Linear}_{\theta'}(1034, 1024) \\
\Theta_{\theta'}^{\text{orient}}(Z, G_R, T) &= \text{SoftMax}(\text{Linear}_{\theta'}(1034, 4))
\end{aligned}$$

$$\begin{aligned}
\mu_{\theta'}^{\text{loc}}(Z, G_R, T) &= \text{Linear}_{\theta'}(1034, 3) \\
\mu_{\theta'}^{\text{size}} &= \text{Linear}_{\theta'}(1024, 512) \rightarrow \text{ReLU} \rightarrow \text{Linear}_{\theta'}(512, 3)
\end{aligned}$$

This is a three-layer MLP with ReLU activations and 1024 input neurons since the input is the mean of the shape features  $\mu_{\theta'}^{\text{shape}}(Z, G_R, T)$ .

$$\Theta_{\theta'}^{\text{cat}} = \text{Linear}_{\theta'}(1024, 512) \rightarrow \text{ReLU} \rightarrow \text{Linear}_{\theta'}(512, 7)$$

The output is 7D since there are 7 super-categories in our dataset, Cabinet/Shelf, Bed, Chair, Table, Sofa, Pier/Stool, Lighting.

$\text{Linear}_{\theta'}(x, y)$  denotes a linear layer with  $x$  input neurons and  $y$  input neurons. Recall  $\theta'$  denotes all the parameters of the Decoder including the GNN and the output MLPs.

## 6.4 Computing the KL divergence term

### 6.4.1 Derivation for (9)

Rewriting (7)

$$\pi^* = \arg \min_{\pi} KL(q_{\phi}(Z \mid G, T, n_F) \parallel p_{\theta''}(Z \mid G_R, \pi, n_F, T)) \quad (13)$$

For simplicity let us denote the two distributions as

$$\begin{aligned}
q_{\phi}(Z \mid G, T, n_F) &= \mathcal{N}(\mu_0, \Sigma_0) \\
p_{\theta''}(Z \mid G_R, \pi, n_F, T) &= \mathcal{N}(\tilde{\pi}\mu_1, \tilde{\pi}\Sigma_1\tilde{\pi}^T),
\end{aligned}$$

where  $\tilde{\pi} = \pi \otimes I_{d_F \times d_F}$ .

The KL divergence between two Gaussian distributions is known analytically,

$$\begin{aligned}
& KL(q_\phi(Z \mid G, T, n_F) \parallel p_{\theta''}(Z \mid G_R, \pi, n_F, T)) \\
&= \frac{1}{2} (Tr(\tilde{\pi} \Sigma_1^{-1} \tilde{\pi}^T \Sigma_0) + (\tilde{\pi} \mu_1 - \mu_0)^T \tilde{\pi} \Sigma_1^{-1} \tilde{\pi}^T (\tilde{\pi} \mu_1 - \mu_0)) \\
&\quad + \frac{1}{2} \left( \ln \left[ \frac{\det(\tilde{\pi} \Sigma_1 \tilde{\pi}^T)}{\det(\Sigma_0)} \right] - n_F d_F \right) \\
&\equiv (Tr(\tilde{\pi} \Sigma_1^{-1} \tilde{\pi}^T \Sigma_0) + (\tilde{\pi} \mu_1 - \mu_0)^T \tilde{\pi} \Sigma_1^{-1} \tilde{\pi}^T (\tilde{\pi} \mu_1 - \mu_0)) \\
&= Tr(\Sigma_1^{-1} \tilde{\pi}^T \Sigma_0 \tilde{\pi}) + \mu_1^T \Sigma_1^{-1} \mu_1 - \mu_1^T \Sigma_1^{-1} \tilde{\pi}^T \mu_0 \\
&\quad - \mu_0^T \tilde{\pi} \Sigma_1^{-1} \mu_1 + \mu_0^T \tilde{\pi} \Sigma_1^{-1} \tilde{\pi}^T \mu_0 \\
&\equiv Tr(\Sigma_1^{-1} \tilde{\pi}^T \Sigma_0 \tilde{\pi}) - \mu_1^T \Sigma_1^{-1} \tilde{\pi}^T \mu_0 - \mu_0^T \tilde{\pi} \Sigma_1^{-1} \mu_1 \\
&\quad + \mu_0^T \tilde{\pi} \Sigma_1^{-1} \tilde{\pi}^T \mu_0 \\
&\equiv Tr(\Sigma_1^{-1} \tilde{\pi}^T \Sigma_0 \tilde{\pi}) - 2\mu_1^T \Sigma_1^{-1} \tilde{\pi}^T \mu_0 + \mu_0^T \tilde{\pi} \Sigma_1^{-1} \tilde{\pi}^T \mu_0
\end{aligned} \tag{14}$$

The third equivalence is obtained by observing that the constant  $n_F d_F$  (which is the dimension of the support of the two Gaussian distributions) does not affect the solution of (13) and that permuting the rows and column of a matrix by the same permutation does not change its determinant and hence the minimizer  $\pi^*$  will also not depend on this term. By similar reasoning, we also ignore the factor of  $\frac{1}{2}$ . In the fifth equivalence we again ignore terms that don't affect  $\pi^*$ . Using the cyclic property of the *Trace* operator we can rewrite the last term on the RHS of (14) as

$$\mu_0^T \tilde{\pi} \Sigma_1^{-1} \tilde{\pi}^T \mu_0 = Tr(\mu_0^T \tilde{\pi} \Sigma_1^{-1} \tilde{\pi}^T \mu_0) = Tr(\Sigma_1^{-1} \tilde{\pi}^T \mu_0 \mu_0^T \tilde{\pi})$$

Substituting this results in (14) we obtain the desired result.

$$\begin{aligned}
& KL(q_\phi(Z \mid G, T, n_F) \parallel p_{\theta''}(Z \mid G_R, \pi, n_F, T)) \\
&\equiv Tr(\Sigma_1^{-1} \tilde{\pi}^T \Sigma_0 \tilde{\pi}) - 2\mu_1^T \Sigma_1^{-1} \tilde{\pi}^T \mu_0 + Tr(\Sigma_1^{-1} \tilde{\pi}^T \mu_0 \mu_0^T \tilde{\pi}) \\
&= Tr(\Sigma_1^{-1} \tilde{\pi}^T [\Sigma_0 + \mu_0 \mu_0^T] \tilde{\pi}) - 2\mu_1^T \Sigma_1^{-1} \tilde{\pi}^T \mu_0 \\
&= Tr(\Sigma_1^{-1} \tilde{\pi}^T [\Sigma_0 + \mu_0 \mu_0^T] \tilde{\pi}) - 2Tr(\mu_1^T \Sigma_1^{-1} \tilde{\pi}^T \mu_0) \\
&= Tr(\Sigma_1^{-1} \tilde{\pi}^T [\Sigma_0 + \mu_0 \mu_0^T] \tilde{\pi}) - 2Tr(\tilde{\pi}^T \mu_0 \mu_0^T \Sigma_1^{-1})
\end{aligned}$$

We again used the cyclic property of the *Trace* operator for the last equality. This concludes our derivation for (9).

#### 6.4.2 Solving (9) using the FAQ approximation

. The FAQ algorithm proceeds as follows,

1. **Choose an initial point:** We choose the uninformative  $\pi_0 = \frac{1 \cdot 1^T}{n_F}$  as the initial estimate for the algorithm. Note, here  $\pi^0$  is a doubly stochastic matrix and not a permutation matrix.
2. **Find a local solution:** In each iteration  $i$ , we linearize the objective at the current iterate  $\pi^i$

$$\tilde{f}^i(\pi) := f(\pi^i) + Tr[\nabla f(\pi^i)^T (\pi - \pi^i)]$$

Here,  $f(\pi) = Tr(\Sigma_1^{-1} \tilde{\pi} [\Sigma_0 + \mu_0 \mu_0^T] \tilde{\pi}^T) - 2Tr(\tilde{\pi} \mu_0 \mu_0^T \Sigma_1^{-1})$ . We then solve the following subproblem

$$\begin{aligned}
& \min_{\pi} Tr(\nabla f(\pi^i)^T (\pi - \pi^i)) \\
& \text{s.t. } \pi \in D
\end{aligned} \tag{15}$$

Here  $D$  is the set of all doubly stochastic matrices. Notice (15) is just a Linear Assignment Problem and can be efficiently solved by the Hungarian Algorithm. Let  $q^i$  denote the arg min of (15).

3. **Choose the next iterate:** Finally choose  $\pi^{i+1} = \alpha \pi^i + (1 - \alpha) q^i$ , where  $\alpha \in [0, 1]$ . Here  $\alpha$  is chosen by solve the 1D optimization problem analytically.

$$\min_{\alpha} f(\alpha \pi^i + (1 - \alpha) q^i) \quad \text{s.t. } \alpha \in [0, 1] \tag{16}$$



4. **Repeat steps 2 and 3 untill convergence.** Steps 2-3 are repeated iteratively untill some termination criteria is met, say  $\|\pi^i - \pi^{i-1}\|_F < \epsilon$ . In practice, we do not run steps 2-3 untill convergence but terminate after just 1 iteration of the FAQ algorithm. Running for longer iterations did not result in any significant gains in performance.
5. **Project onto the set of permutation matrices.** Upon termination, the final solution is obtained by projecting  $\pi^{final}$  onto the space of permutation matrices by solving  $\min_{\pi \in P} -Tr(\pi^{final} \pi^T)$ . Here  $P$  is the set of all permutation matrices of size  $n_F$ . This is against solved by the Hungarian Algorithm.

In step 2, we need to compute the gradient of  $f(\pi^i)$ . This can be done analytically. We will start our derivation by stating some facts. First, the gradient of the dot product of two matrices  $A$  and  $X$  with respect to  $X$  is,

$$\frac{d}{dX} \langle A, X \rangle = A \quad (17)$$

Second, for every linear operator  $M$ , its adjoint operator  $M^\dagger$  is defined such that

$$\langle A, M(X) \rangle = \langle M^\dagger(A), X \rangle \quad (18)$$

Recall,

$$f(\pi) = Tr(\Sigma_1^{-1} \tilde{\pi} [\Sigma_0 + \mu_0 \mu_0^T] \tilde{\pi}^T) - 2Tr(\tilde{\pi} \mu_0 \mu_1^T \Sigma_1^{-1})$$

We will first look at the second term,

$$\begin{aligned} Tr(\tilde{\pi} \mu_0 \mu_1^T \Sigma_1^{-1}) &= \langle \Sigma_1^{-1} \mu_1 \mu_0^T, M(\pi) \rangle \\ &= \sum_{ij}^{n_F \times n_F} \pi_{ij} Tr([\Sigma_1^{-1} \mu_1 \mu_0^T]_{ij}) \\ &= \langle M^\dagger(\Sigma_1^{-1} \mu_1 \mu_0^T), \pi \rangle \end{aligned} \quad (19)$$

Here,  $M(\pi) := \pi \otimes I_{d_F \times d_F}$ . Given a matrix  $A \in \mathbb{R}^{n_F d_F \times n_F d_F}$ , we define the operation  $[A]_{ij}$  (used in the second equality) as follows. First divide the matrix  $A$  into non-overlapping blocks of size  $d_F \times d_F$ , there are  $n_F \times n_F$  such blocks. Now  $[A]_{ij}$  denotes the  $ij^{th}$  block. In the last equality, we defined the adjoint  $L^\dagger(A)$  as  $\hat{A}$ . Here  $\hat{A}$  is a  $n_F \times n_F$  matrix obtained from  $A$  whose  $ij^{th}$  entry is,

$$\hat{A}_{ij} = Tr([A]_{ij}).$$

Combining (19) with (17) we conclude

$$\frac{d}{d\pi} Tr(\tilde{\pi} \mu_0 \mu_1^T \Sigma_1^{-1}) = M^\dagger(\Sigma_1^{-1} \mu_1 \mu_0^T) \quad (20)$$

The gradient of the first term is calculated similarly,

$$\begin{aligned} Tr(\Sigma_1^{-1} \tilde{\pi} [\Sigma_0 + \mu_0 \mu_0^T] \tilde{\pi}^T) &= \langle \Sigma_1^{-1} \tilde{\pi} [\Sigma_0 + \mu_0 \mu_0^T], M(\pi) \rangle \\ \frac{d}{d\pi} Tr(\Sigma_1^{-1} \tilde{\pi} [\Sigma_0 + \mu_0 \mu_0^T] \tilde{\pi}^T) &= 2M^\dagger(\Sigma_1^{-1} \tilde{\pi} [\Sigma_0 + \mu_0 \mu_0^T]) \end{aligned} \quad (21)$$

Here  $M(\pi)$  is again defined as  $\pi \otimes I_{d_F \times d_F}$ . Putting it all together,

$$\nabla f(\pi) = 2M^\dagger(\Sigma_1^{-1} \tilde{\pi} [\Sigma_0 + \mu_0 \mu_0^T]) - 2M^\dagger(\Sigma_1^{-1} \mu_1 \mu_0^T) \quad (22)$$

## 6.5 Learning Under Constraints

Let furniture graph  $G_F$  be the input to the encoder and  $\tilde{G}_F$  be the furniture graph reconstructed by the decoder. Recall,  $E_{FF}$  denotes the edges between furniture nodes in  $G_F$  (Section 3.1) and  $\tilde{G}_F$  has the same structure as  $G_F$ . We employ the following constraints,

- **furniture-furniture distance constraint:** For every  $(v_i, v_j) \in E_{FF}$ , we define their relative position as  $c_{ij} = \|loc(v_i) - loc(v_j)\|_2$ , where  $loc(v_i)$  denotes the 3D centroid of furniture item  $v_i$  from  $G_F$ . We define  $c_{ij}^{pred} = \|loc^{pred}(v_i) - loc^{pred}(v_j)\|_2$  as the relative distance computed from the corresponding location mean prediction by the decoder from  $\tilde{G}_F$ . Finally we define  $d_{FF}^{ij} := MSE(c_{ij}, c_{ij}^{pred})$ . Here  $MSE$  refers to mean squared error.
- **furniture-room distance constraint:** This constraint restricts the relative position of the predicted furniture items with the room nodes.
  - For the windows and doors,  $d_{RF}^{ij}$  is defined analogously as  $d_{RF}^{ij} = MSE(c_{ij}, c_{ij}^{pred})$  where  $(v_i, v_j) \in E_{RF}$ , with the exception that for computing  $c_{ij}^{pred}$  we use the ground truth room node location since they are not predicted by the decoder.
  - For walls,  $c_{ij}^{pred}$  is computed as the signed distance between the  $i^{th}$  wall node and the  $j^{th}$  furniture centroid. This ensures the decoder predicts furniture items on the correct side of the wall.
- **furniture-furniture relative orientation constraint:** This constraint enforces the relative orientation between two predicted furniture centroid locations to be close to the ground truth. Specifically we define  $\forall (v_i, v_j) \in E_{FF} o_{FF}^{ij} = orient(v_i, v_j)^T orient^{pred}(v_i, v_j)$ . Here  $orient(v_i, v_j)^T$  is the unit vector pointing in the direction  $loc(v_i) - loc(v_j)$  computed from  $G_F$ . Similarly,  $orient^{pred}(v_i, v_j)$  is the unit vector pointing in the direction  $loc^{pred}(v_i) - loc^{pred}(v_j)$  computed from the reconstruction  $\tilde{G}_F$ .

We now present the complete optimization objective as

$$\begin{aligned}
& \max_{\theta', \theta'', \phi} \mathcal{L}(\theta', \theta'', \phi) \\
& s.t. \quad \frac{1}{n} \sum_{i=1}^n \left[ \sum_{(v_i, v_j) \in E_{FF}} d_{FF}^{ij} \right] \leq \epsilon \\
& s.t. \quad \frac{1}{n} \sum_{i=1}^n \left[ \sum_{(v_i, v_j) \in E_{RF}} d_{RF}^{ij} \right] \leq \epsilon \\
& s.t. \quad \frac{1}{n} \sum_{i=1}^n \left[ \sum_{(v_i, v_j) \in E_{FF}} o_{FF}^{ij} \right] \geq 1 - \epsilon
\end{aligned} \tag{23}$$

Here  $\epsilon$  is a user-defined hyperparameter that determines the strictness of enforcing these constraints<sup>3</sup>.

$\mathcal{L}(\theta', \theta'', \phi)$  is as defined in (2) and  $i$  is in iterator over the scene graphs in the training set. We employ the learning under constraints framework introduced by Chamon und Ribeiro (2020) which results

---

<sup>3</sup>One could also have used a different  $\epsilon_i$  per constraint.

in a primal-dual saddle point optimization problem. For completeness, we will now describe this algorithm in detail. We begin by explicitly writing out the empirical lagrangian  $\hat{\mathcal{L}}_{\theta', \theta'', \phi, \lambda_1, \lambda_2, \lambda_3}$ ,

$$\begin{aligned}
g_1(\theta', \theta'', \phi) &:= \frac{1}{n} \sum_{i=1}^n \left[ \sum_{(v_i, v_j) \in E_{FF}} d_{FF}^{ij} \right] \\
g_2(\theta', \theta'', \phi) &:= \frac{1}{n} \sum_{i=1}^n \left[ \sum_{(v_i, v_j) \in E_{RF}} d_{RF}^{ij} \right] \\
g_3(\theta', \theta'', \phi) &:= \frac{1}{n} \sum_{i=1}^n \left[ \sum_{(v_i, v_j) \in E_{FF}} o_{FF}^{ij} \right] \\
\hat{\mathcal{L}}_{\theta', \theta'', \phi, \lambda_1, \lambda_2, \lambda_3} &:= \mathcal{L}(\theta', \theta'', \phi) + \lambda_3(1 - \epsilon - g_3(\theta', \theta'', \phi)) \\
&\quad + \lambda_1(g_1(\theta', \theta'', \phi) - \epsilon) + \lambda_2(g_2(\theta', \theta'', \phi) - \epsilon)
\end{aligned} \tag{24}$$

Here  $\lambda_1, \lambda_2, \lambda_3$  are the dual variables. The empirical dual problem is then defined as,

$$\hat{D}^* := \max_{\lambda_1, \lambda_2, \lambda_3} \min_{\theta', \theta'', \phi} \hat{\mathcal{L}}_{\theta', \theta'', \phi, \lambda_1, \lambda_2, \lambda_3}.$$

It was shown in Chamon und Ribeiro (2020) that a saddle-point optimization of this empirical dual will give an approximate solution to (23). Algorithm 1 describes the exact steps. At step 5 we require a  $\rho$ -optimal minimizer to the empirical Lagrangian, in practice this is done by running the ADAM optimizer for one epoch. After each epoch  $t$ , the dual variables are updated depending on the slack evaluated with current parameters  $(\theta'^{(t-1)}, \theta''^{(t-1)}, \phi^{(t-1)})$ . At an intuitive level, the algorithm is similar to regularized optimization with adaptive Lagrange multipliers (the dual variables). In (24) each term after  $\mathcal{L}(\theta', \theta'', \phi)$  can be thought of a regularizer (one corresponding to each constraint). The Lagrange multipliers are updated in each epoch to enforce or relax the regularizer depending on whether the corresponding constraint is violated or satisfied.

---

**Algorithm 1** Learning under constraints

---

**Require:** *Initializations:*  $\theta'^{(0)}, \theta''^{(0)}, \phi^{(0)}$ ; *Learning rate for dual variables*  $\eta$ ; *Number of steps*  $T$

- 1:  $\lambda_1^{(0)} = 0$
- 2:  $\lambda_2^{(0)} = 0$
- 3:  $\lambda_3^{(0)} = 0$
- 4: **for**  $t = 1, \dots, T$  **do**
- 5:   Obtain  $\theta'^{(t-1)}, \theta''^{(t-1)}, \phi^{(t-1)}$  such that,

$$\hat{\mathcal{L}}_{\theta', \theta'', \phi, \lambda_1, \lambda_2, \lambda_3} \leq \min_{\theta', \theta'', \phi} \hat{\mathcal{L}}_{\theta', \theta'', \phi, \lambda_1, \lambda_2, \lambda_3} + \rho.$$

- 6:   Update dual variables

$$\begin{aligned}
\lambda_1^{(t)} &= \left[ \lambda_1^{(t-1)} + \eta(g_1(\theta'^{(t-1)}, \theta''^{(t-1)}, \phi^{(t-1)}) - \epsilon) \right]_+ \\
\lambda_2^{(t)} &= \left[ \lambda_2^{(t-1)} + \eta(g_2(\theta'^{(t-1)}, \theta''^{(t-1)}, \phi^{(t-1)}) - \epsilon) \right]_+ \\
\lambda_3^{(t)} &= \left[ \lambda_3^{(t-1)} + \eta(1 - \epsilon - g_3(\theta'^{(t-1)}, \theta''^{(t-1)}, \phi^{(t-1)})) \right]_+
\end{aligned}$$

- 7: **end for**
- 

In Figure 5, we show training curves for ELBO objective (3) and the ELBO objective with constraints (23) which clearly show the benefit of using constraints. Empirically on the 3D-FRONT dataset, getting good solutions is impossible (even after 900 epochs (70k iterations)) without using constraints. The network performance without any constraints is comparable, to that with constraints, for the furniture category, shape and size loss terms. These are arguably much easier to learn than the orientation and position in 3D.

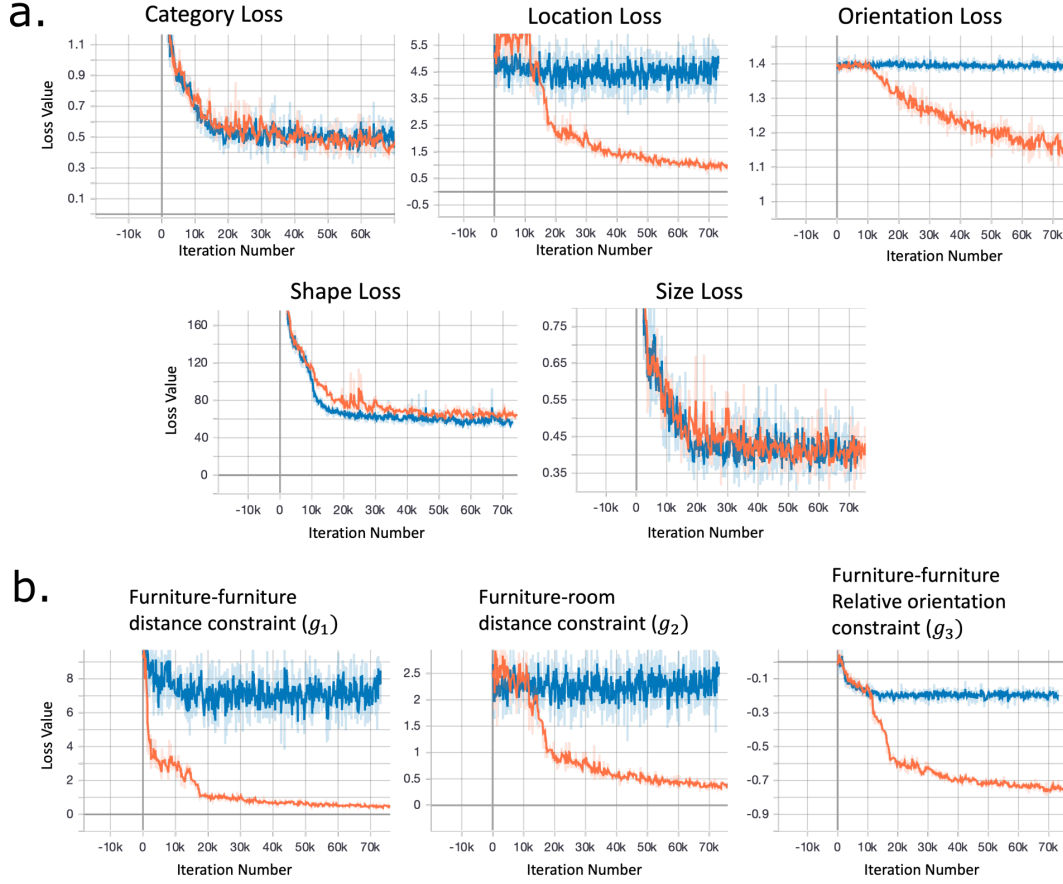


Figure 5: *Ablation studies showing the effect of constraints on training. The orange curve indicates learning under constraints whereas the blue curve indicates learning without any constraints*(a) Training curves for the terms in the reconstruction loss of the ELBO (first term in (3)); (b) Objective values of the constraints as training progresses. Note the x-axis is the number of iterations rather than epoch (one iteration is one batch processed).

## 6.6 Diverse furniture layout recommendations for the same room layout

More examples for Figure 1b in Figure 6

## 6.7 More Examples for Figure 3

### 6.7.1 Manipulating Latent Space

See Figure 7

### 6.7.2 Interpolating along the latent space

See attached videos. “Interpolation\_3.mp4” contains a finer discretization of the example in Figure 3c. Refer to the last paragraph of “Manipulating the Latent space” in section 3.2 for details on how these videos were generated.

## 6.8 Analyzing matched furniture nodes for the trained model

We analyzed the ordering of the matched furniture items for our trained model by carrying out the following steps,



Figure 6: **Diverse furniture layout recommendations for the same room layout.** Each row depicts a specific room, row 1,2 : living room; row 3,4,5 bedroom. The first column is the ground truth layout from the test set. The remaining columns are recommendations made by our proposed model. All rooms are top-down rendering of the scene except the first row which was generated using blender. The two black boxes marked asterisk in row 4 and 5 are ceiling lights. Notice how sometimes the network proposes a different room type given that is still a reasonable layout. For example, row 4, column 5, the network proposes a living room setup with a sofa instead of a bedroom. Similarly, row 5 column 4, the network proposes the library with a book shelf and a chair instead of a bedroom.

- Iterate over the scenes in the test set.
- Every scene is a tuple consisting of the attributed scene graph, the room type and the number of furniture's in the room  $(G, T, n_F)$ . For each scene,
  - Pass it through the trained GNN encoder to obtain the parameters for  $q_\phi(Z | G, T, n_F)$ . Here  $Z := \{Z^1, Z^2, \dots, Z^{n_F}\}$  is the set of latent variables corresponding to the  $n_F$  furniture items to be placed in the room.
  - Next solve (7) using the FAQ algorithm and the Graph prior  $p_{\theta''}(Z | G_R, \pi, T, n_F)^4$  to find the optimal ordering  $\pi^*$ . Here  $G_R$  refers to the room layout graph derived from the input scene graph.
  - This  $\pi^*$  is the optimal assignment between  $Z_i$ 's obtained from the approximate posterior  $q_\phi(Z | G, T, n_F)$  and the sequential latent nodes sampled using the auto-regressive prior (See (5)).

<sup>4</sup>Recall, given any ordering of the latent variables,  $\pi$ , the Graph Prior simulates an auto-regressive model based on  $\pi$ . See (6)

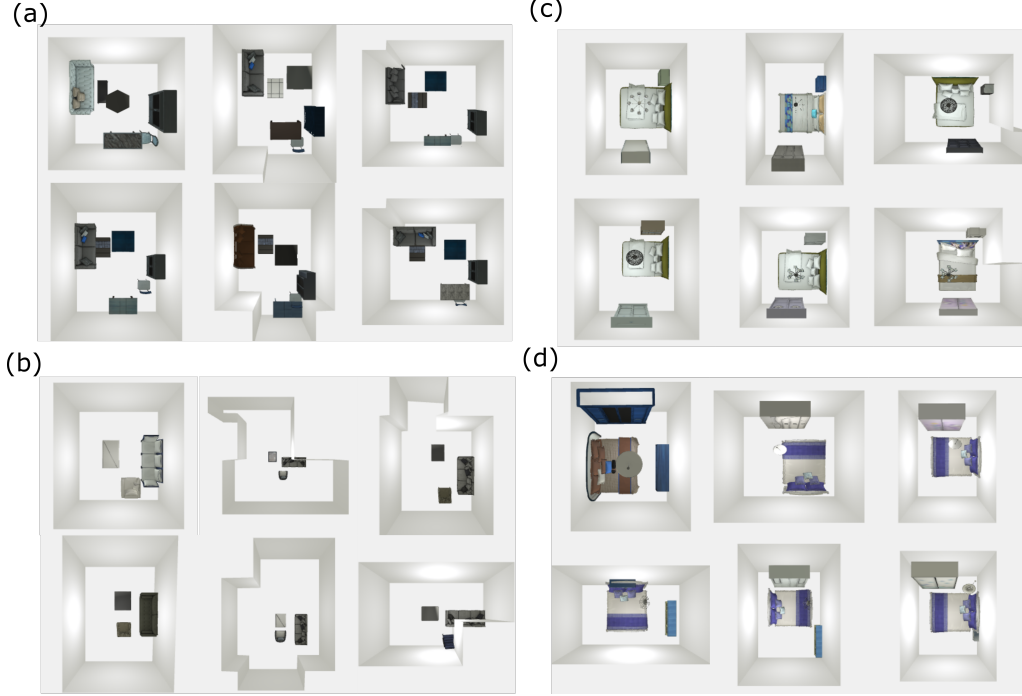


Figure 7: **Manipulating the latent space.** We show recommendations made by our model for different rooms using the posterior distribution obtained from the test set furnished room. In all four figures the first image corresponds to the rendering of a test set indoor scene. Notice how the network orients the sofa (in (a) and (b)) and the bed (in (c) and (d)) to account for the room structure.

Table 5: Frequency of categories mapped to the first latent sampled by the auto-regressive prior

Categories	Bedroom	Livingroom
Bed	0.30	0.0
Light	0.19	0.19
Night-stand	0.43	0.0
Chair	0.02	0.11
Sofa	0.01	0.20
Table	0.04	0.10
Pier	0.01	0.01
Coffee-Table	0.0	0.39

- Since each  $Z_i$  corresponds to a furniture item, we analyze the frequencies (over the test set) with which a certain category is mapped to the first latent sampled by the auto-regressive prior. This can give insights into what the model has learnt and whether the prior’s modelling of furniture placement in indoor scenes correlates with how interior designers begin planning room layouts. In Table 5 we present these results. We found that the first bedroom item matched by our model is a nightstand/bed/light with probability 0.91 and the first living room item matched is a coffee-table/sofa/light with probability 0.76. This is interesting since human designers often start planning with these items.